

Deploying Public Charging Stations for Battery Electric Vehicles on the Expressway Network Based on Dynamic Charging Demand

Tian-Yu Zhang^{ID}, Yang Yang^{ID}, Yu-Ting Zhu, En-Jian Yao^{ID}, and Ke-Qi Wu

Abstract—There is an obvious gap between the rapid growth of battery electric vehicle (BEV) intercity travel demand and the worse deployment of charging facilities on the expressway network. With the consideration of dynamic charging demand, a bilevel model is proposed to deploy charging stations for the expressway network. The upper model aims at determining the location of charging stations and the number of chargers in each station to minimize the construction cost and total BEV travel cost. The dynamic charging demand is obtained by the lower model, which is constructed as a multiclass dynamic traffic assignment model, including charging, queuing, and flow transmission processes. A genetic algorithm incorporating the method of successive averages is adopted to solve the bilevel model. A real case in the Shandong province of China is employed to evaluate the effectiveness of the proposed model and algorithm. The sensitivity analyses show that a high level of charging service can encourage the usage of BEVs. In addition, when the BEV percentage is at a low level, planners should give priority to the quantity and location to expand charging service coverage and BEV's travel range; then, with the increasing of BEV percentage, the construction emphasis should change to charging station's capacity.

Index Terms—Battery electric vehicle (BEV), bilevel optimization model, deployment model, dynamic traffic assignment (DTA), public charging station.

NOMENCLATURE

Sets

- A_c Set of links with charging station, $A_c \in A$.
- A_k Link set on route k , $A_k = \{a_1, \dots, a_x, \dots, a_N\}$.
- C_k Charging station set on route k , $C_k = \{c_1, \dots, c_i, \dots, c_n\}$, $C_k \in A_k$.
- K_{rs} Set of routes connecting (r, s) .
- K_{rs}^m Set of routes of class m for connecting (r, s) , $K_{rs}^m \in K_{rs}$.

Manuscript received August 30, 2021; revised November 21, 2021; accepted December 24, 2021. Date of publication January 7, 2022; date of current version April 20, 2022. This work was supported by the National Natural Science Foundation of China under Grant 71801012 and Grant 71931003. (Corresponding author: Yang Yang.)

Tian-Yu Zhang, Yang Yang, and En-Jian Yao are with the Key Laboratory of Transport Industry of Big Data Application Technologies for Comprehensive Transport, Beijing Jiaotong University, Beijing 100044, China (e-mail: tianyu_zhang@bjtu.edu.cn; y_yang@bjtu.edu.cn; enjyao@bjtu.edu).

Yu-Ting Zhu is with the School of E-Business and Logistics, Beijing Technology and Business University, Beijing 100048, China (e-mail: zhuyuting@btbu.edu.cn).

Ke-Qi Wu is with the Administrative Approval and Service Centre, Beijing Municipal Commission of Transport, Beijing 100053, China (e-mail: wukeqi@jtw.beijing.gov.cn).

Digital Object Identifier 10.1109/TTE.2022.3141208

P_{c_i}	Charger set of charging station c_i , $P_{c_i} = \{p_{c_i}^1, p_{c_i}^2, \dots, p_{c_i}^j\}$.
$\text{EE}(n)$	Set of links whose head node is n .
$\text{ES}(n)$	Set of links whose tail node is n .
m^*	Special GV and BEV entering the route k during interval t , $m^* = \{g^* =_{rs,k}^{g,t}, e^* =_{rs,k}^{e,t}\}$.

Parameters

S_1	Lower bound of SOC during the trip.
S_2	Lower bound of SOC when leaving the network.
U	Voltage of electric battery (V).
Q	Capacity of electric battery (A·h).
$t_{a_x}^m$	Free-flow travel time of type m on link a_x .
LC_{a_x}	Capacity of link a_x .
a^m	Convert coefficient of the vehicle of type m .
$\alpha^{rs,m}$	Travel time value of vehicles of type m on OD pair (r, s) .
$\beta^{rs,m}$	Energy consumption value of vehicles of type m on OD pair (r, s) .
$\gamma^{rs,m}$	Charging/waiting time value of vehicles of type m on OD pair (r, s) .
θ	Discrete coefficient, reflecting the perception difference of travelers.
$M_{rs,k}$	Correction term of route k on OD pair (r, s) in the PSL model.
l_{a_x}	Length of link a_x .
$l_{rs,k}$	Length of route k on OD pair (r, s) .
N_{\min}	Lower bound of charger's number in one charging station.
N_{\max}	Upper bound of charger's number in one charging station.

Auxiliary Variables of Charging Simulation

$S_n^{e*,t}$	SOC of e^* reaching node n at time t .
$H_{n_1,n_2}^{e,t}$	Energy consumption of BEV from node n_1 to node n_2 at time t .
$H_{a_x}^{e,t}$	Energy consumption of EV through link a_x at time t .
$T_{p_{c_i}^j}^t$	Remaining working time (RWT) of the charger $p_{c_i}^{*,t}$.
$p_{c_i}^{*,t}$	Charger with minimum RWT in charging station c_i at time t .
$t_{wc_i}^{e*}$	Waiting time of e^* in charging station c_i at time t .

t_{cc}^{e*}	Charging time of e^* in charging station c_i at time t .
t_{sc}^{e*}	Total service time of e^* in charging station c_i at time t .
<i>Auxiliary Variables of Route Choice Model</i>	
$\tau_{ax}^{m,t}$	Travel time of vehicles of type m on link a_x at time t .
q_{ax}^t	Queue length of link a_x at time t .
$\tau_k^{m,t}$	Travel time of vehicles of type m on route k .
TC_{m*}	Generalized travel cost of vehicle m^* .
$\delta_{rs,k}^{ax}$	Binary variable: 1 indicates that link a_x is part of route k on OD pair (r, s) , 0 otherwise.
$\rho_{rs,k}^{ax}$	Binary variable: 1 indicates that charging station c_i is part of route k on OD pair (r, s) , 0 otherwise.
r_0^{e*}	Binary variable: 1 indicates that the original route k on OD pair (r, s) without charging demand is an effective alternative route for BEV e^* , 0 otherwise.
$r_{c_i}^{e*}$	Binary variable: 1 indicates that the route k on OD pair (r, s) where BEV charges at station c_i are an effective alternative route for BEV e^* , 0 otherwise.
$P_{rs,k}^{m,t}$	Choosing probability of route k for vehicles of type m at time t .
f_{m^*}	New loading traffic volume of route k for vehicle m^* at time t .
$q_{rs}^{m,t}$	New loading traffic volume of the vehicle on OD pair (r, s) at time t .

Auxiliary Variables of Dynamic Network Loading

X_a^t	Occupancy of link a at time t .
$X_a^{m,t}$	Occupancy of link a of the vehicle of type m at time t .
$v_a^{m,t}$	Flow rate of entering link a at time t .
$u_a^{m,t}$	Flow rate of leaving link a at time t .
$v_{rs,k}^{m,t}$	Inflow rate of choosing route k on OD pair (r, s) at time t .
$u_{rs,k}^{m,t}$	Outflow rate of choosing route k on OD pair (r, s) at time t .
d_a^t	Occupancy of charging station c at time t .

Auxiliary Variables of Upper Model

\mathbf{v}	Link flow vector.
\mathbf{f}	Route flow vector.
\mathbf{y}	Layout of charging station.
$Z(\mathbf{y})$	Total objective cost under the layout \mathbf{y} .
$Z_{con}(\mathbf{y})$	Construction cost under the layout \mathbf{y} .
$Z_{tra}(\mathbf{y})$	Total travel cost of BEV under the layout \mathbf{y} .
B_1	Construction cost of the charging station at location i .
B_2	Construction cost of the charger at location i .
B^*	Upper threshold of the construction cost.
ω_1	Coefficient of the construction cost.
ω_2	Coefficient of the total BEV travel cost.
ϕ	Set of the existing expressway service areas.

Decision-Making Variables of Upper Model

- y_i Binary variable, which equals 1 when a charging station is built at location i ; otherwise, it equals 0.
- p_i Number of chargers at station i .

I. INTRODUCTION

IN THE face of climate deterioration and energy crisis, transportation electrification is significant in promoting the proportion of electric energy in transportation terminal consumption, building a resources recycling system, and improving the deep integration of electrified transportation and energy systems. With the innovation in battery technologies, the support in government policies, and the increase in social acceptability, the number of private battery electric vehicles (BEVs) has been increasing in the past several years. It has exceeded 5.51 million at the end of March 2021 [1]. By 2025, the number of BEVs is planned to reach 25 million [2].

With the improvement of BEV driving range and charging facilities' power, and the development of urban agglomeration, the potential intercity travel demand of BEVs is increasing. The reasonable layout of charging facilities on the expressway network is an essential basis for improving the travel accessibility of BEVs and promoting the BEV market. However, there is still an obvious gap between the rapid growth of BEVs' intercity travel demand and the worse deployment of charging facilities on the expressway network. On the one hand, the construction scale of charging stations on the expressway is small and needs to be expanded. By the end of 2018, there were only 1800 charging stations with 7500 chargers on the expressway in China [3]. The 14th five-year development plan for the integrated transport services in China clearly points out accelerating the construction of charging infrastructure [4]. On the other hand, without an appropriate deployment strategy, the utilization rates of charging facilities are imbalanced. Most of the chargers are idle all the time, and the utilization rates are less than 15% [5]. Only a few are fully utilized. These phenomena prompt governments and researchers to focus on the deployment problem of chargers on the expressway network, including the scale and the location of charger stations.

Charging demand is one of the fundamentally important inputs for the deployment problem of charging stations. Considering drivers' favor of choosing chargers near the origin or destination of a trip [6], a simple way is to assume that charging demand is fixed and only occurs in the origin or destination area [7]–[9]. However, this kind of simplified is only suitable for a short-distance trip, i.e., intraurban travel: the cruising range of BEVs can cover the whole trip. For an intercity travel, since the cruising range of BEV is shorter than the whole length of the trip, at least one charging demand is needed during the travel.

To obtain the charging demand during travel, a traffic assignment model is employed by charging station deployment researchers [10]–[14]. Then, the charging demand of a charger can be obtained based on the result of traffic assignment, namely, equals to the number of BEVs assigned to the path with a charging behavior in this charger. However, assignment results in these studies are fixed and calculated based on hourly

or daily origin-destination (OD) travel demand matrices at the beginning of the study period. The time-varying feature of travel demand and the changeable feature of drivers' choice behavior are rarely considered.

In fact, the time-varying feature of travel demand and the changeable feature of drivers' choice behavior are widespread in transportation systems. Previous studies about drivers' choice behavior indicated that travel demands on an expressway network are obviously different at different times [15]–[17]. Drivers' charging and path choice results are always determined based on the location of chargers [18]–[22] and changed based on the choice behavior of others dynamically [23]–[25]. If a charging deployment model does not consider these two kinds of features, charging demand cannot be analyzed accurately, and the effectiveness of the optimized results may reduce greatly.

This article aims to provide a more accurate and practical deployment model for charging stations with the consideration of dynamic charging demand on the expressway network. A real case network in the Shandong province of China is tested by the proposed model and algorithm. Some planning suggestions are given based on the results of the case study. The main contributions of this article are summarized as follows.

This article captures the dynamic charging demand by DTA-based simulation based on the dynamic traffic OD demand with 15 min or fewer time intervals. The DTA-based simulation links the interaction between the BEV driver's charging preference, the real-time traffic network's congestion, the real-time charging facilities' working status by simulating the route choice behavior, the charging service process, and the flow transmission. Compared with the static traffic assignment (STA), the DTA-based deployment model is demonstrated to be effective and effective in estimating the spatial-temporal distribution of demand and capturing the real-time working status of vehicles, charging facilities, and traffic networks.

This article simulates the BEV charging process during the trip dynamically to monitor the real-time level of service (LOS) and working status of charging facilities. With a long charging time (sometimes may reach 30 min), the charging station's working status would directly affect BEV drivers' travel behavior [26]. Hence, obtaining the real-time charging time, waiting time, and travel energy consumption of each route provides a foundation to analyze drivers' changeable travel behavior and capture the real-time charging demand. Considering the feature of energy consumption during the trip on the expressway network, the BEV waiting and charging process in the service area is modeled by queue theory and embedded into the DTA-based simulation.

A bilevel optimization model is proposed for the public charging facilities deployment on the expressway with full consideration of dynamic charging demand. The upper level model is the charging station deployment model to optimize the charging station's location and capacity. The lower level model is a DTA-based model to analyze the dynamic charging process. Then, based on the user equilibrium (UE) result of the lower level model, the dynamic charging demand is obtained and inputted into the upper level model.

The following sections are arranged as follows. The relevant literature about BEV travel behavior, the multiclass dynamic traffic assignment (DTA) model, and the deployment model of charging facilities is discussed in Section II. The problem description, time-expanded network, notation, assumption, and framework are described in Section III. The multiclass DTA model is proposed in Section IV. Then, the charging station deployment model is proposed in Section V. The solution algorithms are shown in Section VI. Section VII is the case study based on an expressway network in Shandong province. Section VIII is conclusions and future research.

II. LITERATURE REVIEW

As an important support for the development of BEVs, the deployment problem of charging infrastructure has received much attention in recent years. The optimization problem is generally described as follows: the deployment tried to improve the user's satisfaction [27]–[29] and reduces the system working load [30], [31] by optimizing the location and the type of charging stations, and the number of chargers. Previous studies can be divided into two different categories: the node-based deployment problem and the flow-based deployment problem.

The node-based deployment model attempts to decide where to locate public charging stations to satisfy charging demand based on nodes in a spatial network. Two kinds of methods are widely used to obtain charging demand. First, the charging demand of a designated area was simplified into an abstract demand mode by considering the land use [32], electric vehicle ownership [33], parking pattern [34], and other features [35], [36]. Other studies provided a data-driven-based method to estimate the spatial-temporal distribution of charging demand based on vehicle trajectory data and charging facility operation data [37]–[40]. However, the node-based facility location model ignores travel behavior and the traffic flows in the network. Therefore, they are not well suited for charging station deployment problems since demands in this kind of problem are flows of BEVs in a network. By recognizing this feature, some researchers try to provide the flow-based deployment model.

The flow-based deployment model, which is widely used in previous studies [41], [42], is inspired by the flow-capturing location-allocation models [43]. Since it considers vehicles' travel process and can deal with the microscopic phenomenon on the network (such as network congestion, vehicle user's route choice behavior, and charging behavior), the flow-based facility location model can capture the charging demand during the flow transmission. With the good performance in simulating traffic flow travel and charging behavior, the STA-based method has been widely adopted to calculate traffic flows for these models. He *et al.* [12] provided a UE-based STA model considering the charging time, range limits, and given the charging-decision variable as the lower model. The upper model of their paper was to optimize the positions of charging stations. To optimize the location of charging stations in urban, Huang and Kockelman [13] proposed an STA model to capture the influence of congested networks and charging stations on drivers' route choice and charging

decisions. To analyze infrastructure deployments under the urban network with BEV flow in the different initial status of charge (SOC) and risk-taking attitudes, He *et al.* [10] developed a bilevel mathematical program where a tour-based network assignment model calculated the charging demand. Considering the travel and charging process, the problem of charging demand during the trip can be solved by STA-based flow-capturing deployment models. However, these models cannot accurately capture the time-variant characteristics of traffic state and charging facilities' operating status, which will influence charging demand significantly [23]–[25].

Focusing on dynamic traffic processes, DTA analyzes the optimal traffic flow distribution based on the real-time traffic demand and supply. Compared with STA, DTA has illustrated that excellent microperformances in traffic simulation: 1) can simulate the process of traffic flow propagation in the network from spatial and temporal dimensions, e.g., network congestion and the distribution of vehicles [44], [45]; 2) can capture and analyze the multiuser travel behavior accurately, e.g., the route choice and charging judgment [46]–[48]; and 3) some traffic phenomena that have an intrinsic dynamic nature, such as charging stations operation, can be simulated [49], [50].

Therefore, to capture the real-time charging demand, this article introduces the multiclass DTA theory to analyze BEV drivers' dynamic travel and charging behavior. Then, combining the multiclass DTA model, a bilevel model is proposed for the deployment problem of charging stations on the expressway network. Finally, a genetic algorithm incorporating the method of successive averages is applied to solve the proposed bilevel model. The results of the real case show that the proposed model can perform well.

III. PROBLEM DESCRIPTION, ABSTRACTED NETWORK, NOTATION, AND FRAMEWORK

A. Problem Description

This article focuses on the charger deployment problem for an expressway network with mixed traffic demand, including BEVs and gasoline vehicles (GVs). $G(N, A)$ denotes the expressway network. $N = \{R, S\}$ is the set of nodes, including entrance/exit nodes and diverging/merging nodes, $n \in N$. R is the set of origin nodes, including entrance nodes and diverging/merging nodes in which traffic flows onto the studied network, $r \in R$. S is the set of destination nodes, including exit nodes and diverging/merging nodes in which traffic flows of the network, $s \in S$. (r, s) denotes an origin and destination (OD) pair. A is the set of links $a \in A$. $m \in M = \{e, g\}$ denotes the vehicle type, where e refers to BEV and g refers to GV. In this network, the location of expressway service areas is given. To simplify the deployment problem and save the construction cost, charging stations could only be built in the expressway service areas. Then, the objective of this optimization model is to determine which service areas are selected to add charging facilities, as well as how many chargers should be constructed.

As an important input for the charging station's deployment, dynamic charging demand should be discussed first. Based on the description in Section II, the charging demand is

the result of traffic flow assignment. Hence, considering the time-varying travel demand and the changeable route choice behavior, we discretize the study period T into S' parts, and the time interval is $t \in T$. The spatial-temporal distribution of charging demand is obtained based on the dynamic link transmission model and the BEV energy consumption model. The refined travel and charging demands provide data support for monitoring the expressway network's traffic condition and charging facilities' operation status. Furthermore, the electric grid and traffic network dynamically adjust the charging load through the BEV drivers' real-time charging station choice behavior and the DTA iteration.

The aim of this article is to determine the location of charging stations and the number of chargers with the consideration of dynamic charging demand to minimize the total travel cost of BEVs and the construction cost of charging infrastructures. A bilevel model is proposed in the next two sections. In this section, the time-expanded network depicts the BEV travel process considering the charging behavior first. Then, notation and assumption are given. Finally, the framework of the bilevel model is described.

B. Time-Expanded Network

During the vehicles' dynamic traveling and charging process, the temporal information of traffic networks and charging facilities is changeable. Therefore, the time-expanded network method [27] is used to illustrate the dynamic travel process considering BEV charging behavior.

Due to the convenience of the refueling process, this article ignores GVs' refueling process, which means that the dwell time in the service area is 0. For BEV drivers, each charging station can be chosen to charge or not to charge. For BEVs without charging demand and GVs, the network structure is the same. For BEVs with charging demand, we add a virtual edge whose length is determined by the charging service time at the station to illustrate the charging process. Based on the layout of charging stations on the expressway network G , we construct two subnetworks: 1) the subnetwork G_1 for GVs and 2) the subnetwork G_2 for BEVs.

For an original travel process [as shown in Fig. 1(a)]: $r \rightarrow n \rightarrow c_1 \rightarrow c_2 \rightarrow s$, Fig. 1 displays the two corresponding subnetworks. r and s represent the OD. n is one node during the trip. The link between node n and s builds two charging stations c_1 and c_2 . As an example of the route in Fig. 1(b), $r \rightarrow n \rightarrow c_1 \rightarrow c'_1 \rightarrow c_2 \rightarrow s$ is the route for BEVs who charge at station c_1 . The service process in the charging station c_1 is expressed by a virtual edge (red line), in which travel time is equal to the sum of waiting time and charging time. The subnetwork G_1 is shown in Fig. 1(b). Fig. 1(b)–(d) together forms the subnetwork G_2 , where Fig. 1(b) shows the route for BEVs without charging demand, and Fig. 1(c) and (d) shows the two charging routes for BEVs with charging demand.

C. Notation and Assumption

The parameters and variables are shown in the Nomenclature.

Several assumptions are explained as follows.

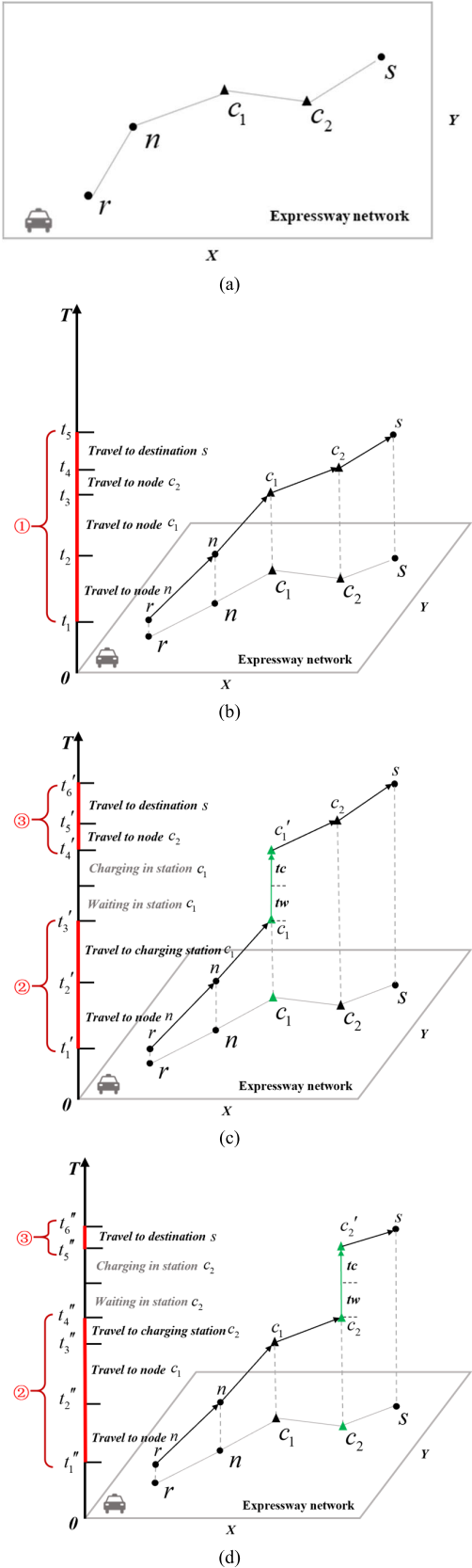


Fig. 1. Time-expanded network for GVs and BEVs. (a) Original travel process. (b) Route for GVs and BEVs without charging demand. (c) Route for BEVs with charging demand in station c_1 . (d) Route for BEVs with charging demand in station c_2 . Note that ①–③ are the travel process with energy consumption, which is explained in Section IV-A.

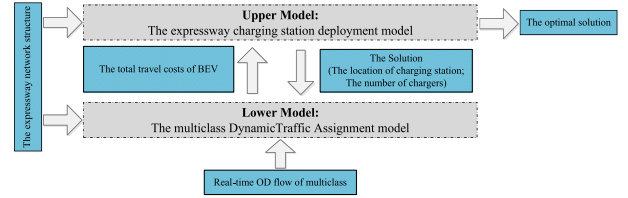


Fig. 2. Framework of research.

Assumption 1: For long trips, drivers usually keep enough power to reduce charging times during the trip. One hypothesis is that BEVs are fully charged at the origin.

Assumption 2: It is assumed that the BEV driver can know in advance what the SOC will be after reaching the next charging station, and the route chosen is the most effective.

Assumption 3: Regardless of users' heterogeneity, it is assumed that all travelers with the same type of vehicle have the same value of time and energy consumption.

Assumption 4: The BEV driver can know the needed waiting time and charging time in each charging station at the departure time and the time of arrival at the charging station.

D. Framework

Considering the time-varying feature of travel and charging demand during the trip, this article proposes a bilevel optimization model for the expressway's public charging facilities' planning. The framework of research is shown in Fig. 2.

With the layout of the charging station coming from the upper model and the real-time multiclass OD flow, the lower model, the link-based multiclass DTA model, is proposed to simulate the multiclass driving and charging behavior. Based on the stochastic UE results, the total travel costs of BEVs are captured, which are the input of the upper model, which is the expressway charging station deployment model. Then, from the perspectives of BEV drivers and facility investors, the upper model optimizes the charging station layout to minimize the BEV travel cost and the charging facilities' construction cost simultaneously and outputs the new solution (the location of stations and the number of chargers in each station).

IV. LOWER MODEL—MULTICLASS DTA MODEL

As the background of the complexed expressway network with public fast-charging stations, a link-based multiclass DTA model [47] is proposed to simulate the BEV and GV travel processes dynamically. As the background of the complex expressway network with public fast-charging stations, a link-based multiclass DTA model [47] is proposed to simulate the BEV and GV travel processes dynamically. Taking the real-time OD flow of multiclass and the expressway network structure as input, the detailed framework of DTA-based simulation is shown in Fig. 3. The core parts of the dynamic simulation can be divided into multiclass route sets' constructing, route choice modeling (RCM), charging simulating, and dynamic network loading (DNL).

First, taking the layout of charging stations and the topological traffic network as input, the available route set of GV is constructed by depth-first search and the Dijkstra algorithm.

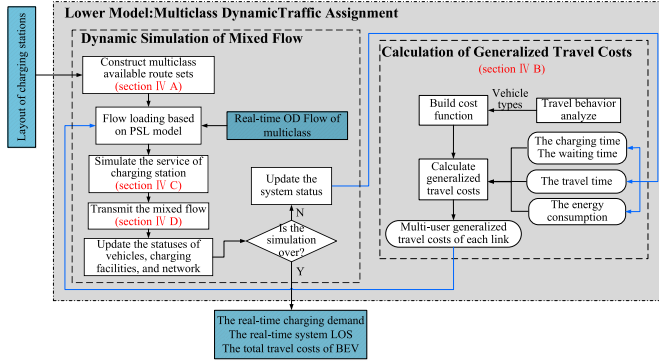


Fig. 3. Framework of DTA-based simulation.

The available route set of EVs satisfying energy consumption constraints is constructed.

Second, the route choice behaviors of GVs and BEVs are modeled based on the path size logit (PSL) model. Under the stochastic dynamic UE (SDUE) principle, the interaction between BEV drivers' route preference and network status is linked dynamically.

Third, based on the queue theory, the charging model simulates the arrived, queuing, charging, and leaving processes of BEVs with energy demand. The real-time operation status of charging facilities is updated for the BEV drivers' charging station choice next time.

Fourth, taking the real-time OD flow and the route cost as input, the mixed flow transmission on the network is simulated based on the link-transmission DTA model. The dynamic traffic network conditions, such as network congestion, are captured for drivers' route choice next time.

A. Multiclass Route Sets' Constructing

It should be noted that the whole transmission of various types of vehicles should satisfy the FIFO principle. Therefore, the independent available route sets of two subnetworks are built. The available route set of G_1 is obtained by depth-first search and the Dijkstra algorithm [17]. For subnetwork G_2 , the route set meeting energy consumption requirements is obtained by calculating the vehicle SOC in each link.

Limited with electric battery capacity, the BEV available route set is determined jointly according to the charging stations' location and the travel route consumption. Considering that after an intercity trip, the BEV needs to reserve enough power for the next trip; the lower bounds of the SOC during the trip and at the destination are introduced, i.e., BEV drivers need to ensure that SOC does not less than S_1 during the trip and above S_2 when leaving the expressway. The BEV available route set meeting energy constraints is constructed as follows

$$r_0^{e^*} = \begin{cases} 1 & S_r^{e^*} - H_{r,s}^{e,t}/(U \cdot Q) > \max(S_1, S_2) \\ 0' & \text{otherwise} \end{cases} \quad (1)$$

$$r_{c_i}^{e^*} = \begin{cases} 1, & [S_r^{e^*} - H_{r,c_i}^{e,t}/(U \cdot Q) > S_1] \\ & \& [S_{c_i}^{e^*} - H_{c_i,s}^{e,t}/(U \cdot Q) > S_2] \\ 0' & \text{otherwise} . \end{cases} \quad (2)$$

As shown in (1), if the energy consumption of the original route [see as the subtrip of ① in Fig. 1(a)] is larger than $\max(S_1, S_2)$, the original route would be available for BEVs without energy demand. For BEVs with charging demand, the original trip is divided into two parts: the trip from the origin to the charging station [see the subtrip of ② in Fig. 1(b) and (c)] and the trip from charging station to destination [see the subtrip of ③ in Fig. 1(b) and (c)]. As shown in (2), if the SOC of BEV e^* arriving at station c_i and the SOC of BEV e^* leaving the network after charging at station c_i are satisfy the energy constraints, the charging route would be available for BEVs.

By constructing the two subnetworks and building independent route sets of BEVs and GVs, two types of vehicles, GVs and BEVs, can follow the FIFO constraint, respectively.

B. Route Choice Modeling

Since drivers generally lack perfect information about traffic network and grid network conditions, the SDUE principle is more relaxed than the UE principle to reflect the route choice behavior [51], [52]. The lower model follows the SDUE principle by introducing the driver's perceptual difference coefficient and a logit model. The RCM obeys the principle of SDUE under the mixed flow of GVs and BEVs, which means that no driver in the mixed network can reduce his/her travel cost by unilaterally changing the travel path [53].

Because different types of vehicle drivers have different choice behaviors, such as charging demands of BEVs, and different understandings of time value and energy consumption value, we will discuss the generalized travel costs of BEVs and GVs, respectively. Then, we describe the route choice behavior of BEVs and GVs based on the PSL model, which is introduced in detail in previous research [54]. The RCM can be described by the PSL model that adds a correction term to the multinomial nest logit (MNL) model to solve the repeat link problem caused by the independence of irrelevant alternative (IIA) feature. The specific formulas of the PSL model are shown as follows:

$$P_{rs,k}^{m,t} = \frac{\exp[-\theta \cdot TC_{rs,k}^{m,t} + \ln(M_{rs,k})]}{\sum_{k \in K_{rs}} \exp[-\theta \cdot TC_{rs,k}^{m,t} + \ln(M_{rs,k})]} \quad \forall r \in O, s \in D, k \in K_{rs}, t \in T, m \in M \quad (3)$$

$$M_{rs,k} = \sum_{a_x \in A_k} \left(\frac{l_{a_x}}{l_{rs,k}} \cdot \frac{1}{\sum_{k \in K_{rs}} \delta_{rs,k}^{a_x}} \right). \quad (4)$$

1) *RCM of BEV*: Based on previous research of BEV travel characters in Section II, its generalized travel cost consists of the travel time, the total service time, and the travel energy consumption.

a) *Travel Time*: We use the cumulative departures (at origin) and arrivals (at destination) to calculate each route's travel time over the time horizon. The calculation formulas for $\tau_{a_x}^{m,t}$, the travel time of vehicles of type m on link a_x at time t , are given as follows:

$$\tau_{a_x}^{m,t} = t_{a_x}^m + q_{a_x}^t / LC_{a_x} \quad \forall a_x \in A_k, t \in T, m \in M \quad (5)$$

$$q_{a_x}^t = \max \left\{ \left[q_{a_x}^{t-1} + T/S' \left(\sum_{m \in M} a^m u_{a_x}^{m,t} - LC_{a_x} \right), 0 \right] \right\} \quad (6)$$

$\forall a_x \in A_k, t \in T$

where $q_{e_n}^t / LC_{e_n}$ is the delay time of link a_x at time t , which is produced by the link congestion and captured by the point queue model. Then, the total travel time $\tau_k^{m,t}$ in route k at time t can be expressed as follows:

$$\tau_k^{m,t} = \tau_{a_1}^{m,t} + \tau_{a_2}^{m,t+\tau_{a_1}^{m,t}} + \cdots + \tau_{a_x}^{m,t+\tau_{a_1}^{m,t}+\cdots+\tau_{a_{x-1}}^{m,t}} \quad \forall k \in K, t \in T, m \in M. \quad (7)$$

b) *Charging Service Time*: The total service time includes the charging time and the waiting time, and the corresponding formulas are (16)–(20).

c) *Travel Energy Consumption*: By introducing vehicle-specific power (VSP), the medium energy consumption model of BEVs is constructed. Based on the average velocity, the BEV energy consumption on link a_x at time t can be calculated by (8). The energy factor $h^e(\bar{v}_{a_x,t})$, referencing [54], can be calculated by (9). The generalized travel cost of BEV e^* can be expressed by (10). BEV e^* traveling on (r, s) at time t and the new loading traffic volume choosing route k can be calculated by (11)

$$H_{a_x}^{e,t} = h^e(\bar{v}_{a_x,t}) \cdot l_{a_x} \quad (8)$$

$$h^e(\bar{v}_{a_x,t}) = 1.359/\bar{v}_{a_x,t} - 0.003\bar{v}_{a_x,t} + 2.981 \times 10^{-5}\bar{v}_{a_x,t}^2 + 0.218 \quad (9)$$

$$\begin{aligned} TC_{e^*} &= \sum_{a_x \in A_k} (\alpha^{rs,e} \cdot \tau_{a_x}^{e,t} + \beta^{rs,e} \cdot H_{a_x}^{e,t}) \cdot \delta_{rs,k}^{a_x} \\ &\quad + \sum_{c_i \in C_k} (t_{wc_i}^{e^*} + t_{cc_i}^{e^*}) \cdot \gamma^{rs,e} \cdot \rho_{rs,k}^{c_i} \cdot r_{c_i}^{e^*} \\ &\quad \forall r \in O, s \in D, k \in K_{rs}^e, t \in T \quad (10) \end{aligned}$$

$$\begin{aligned} f_{e^*} &= q_{rs}^{e,t} \cdot P_{rs,k}^{e,t} = q_{rs}^{e,t} \\ &\quad \cdot \frac{\exp[-\theta \cdot TC_{e^*} + \ln(M_{rs,k})]}{\sum_{k \in K_{rs}} \exp[-\theta \cdot TC_{e^*} + \ln(M_{rs,k})]} \\ &\quad \forall r \in O, s \in D, k \in K_{rs}^e, t \in T. \quad (11) \end{aligned}$$

2) *RCM of GV*: Regardless of GV's refueling time, its generalized travel cost consists of the travel time and the travel energy consumption. Referencing [54], the RCM of GV g^* traveling (r, s) through route k can be described as follows:

$$H_{a_x}^{g,t} = h^g(\bar{v}_{a_x,t}) \cdot l_{a_x} \quad (12)$$

$$h^g(\bar{v}_{a_x,t}) = 125.015/\bar{v}_{a_x,t} - 0.097\bar{v}_{a_x,t} + 9.220 \times 10^{-4}\bar{v}_{a_x,t}^2 + 7.056 \quad (13)$$

$$\begin{aligned} TC_{g^*} &= \sum_{a_x \in A_k} (\alpha^{rs,g} \cdot \tau_{a_x}^{g,t} + \beta^{rs,g} \cdot H_{a_x}^{g,t}) \cdot \delta_{rs,k}^{a_x} \\ &\quad \forall r \in O, s \in D, k \in K_{rs}^g, t \in T \quad (14) \end{aligned}$$

$$\begin{aligned} f_{g^*} &= q_{rs}^{g,t} \cdot P_{rs,k}^{g,t} = q_{rs}^{g,t} \\ &\quad \cdot \frac{\exp[-\theta \cdot TC_{g^*} + \ln(M_{rs,k})]}{\sum_{k \in K_{rs}} \exp[-\theta \cdot TC_{g^*} + \ln(M_{rs,k})]} \\ &\quad \forall r \in O, s \in D, k \in K_{rs}^g, t \in T \quad (15) \end{aligned}$$

where the energy consumption of GV through link a_x at time t can be calculated by (12) and (12); the generalized cost and

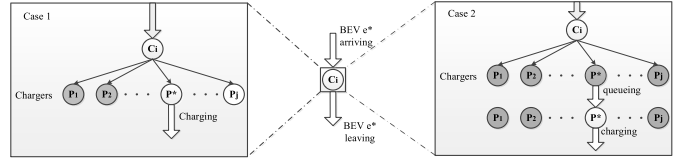


Fig. 4. Charging process and queuing process of BEVs at the charging station.

new loading traffic volume of GV g^* can be calculated by (14) and (15), respectively.

C. Charging Simulating

Based on previous research on BEV charging behavior, the charging model that simulates the arrival, queue, charge, and departure processes of BEV is proposed. The BEV with charging demand needs to wait for charging until one charger is available, which means that the charging service process contains two parts: the queuing process and the charging process.

The total service time includes the queuing time and the charging time. The charging time refers to the time that it takes the BEV to be charged from the current SOC to 100%. Each charging station is equipped with a certain number of chargers, and the charging mode is fast charging, which means that a BEV with 0% power only needs 30 min to be fully charged. Based on J. A. Mas' acceptable current law for battery charging [54], the calculation formula of charging time is shown as follows:

$$t_{cc_i}^{e^*} = 50 \ln[(1 - S_{ci}^{e^*})/0.9371 + 1]. \quad (16)$$

Then, the queuing process is simulated according to the real-time charging stations' status, including the number of chargers and the working status of chargers. In Fig. 4, the shaded circle means that the charger is charging for BEVs, and the blank circle means the idle status. As shown on the left-hand side of Fig. 4, when a charger is idle in the charging station c_i at time t , which means that $T_{p_{c_i}^{*,t}}^t = 0$, the arriving BEV does not need to wait. As shown on the right-hand side, when all chargers in the charging station c_i at time t are occupied, which means that $T_{p_{c_i}^{*,t}}^t > 0$, the BEV with charging demand needs to wait until one is free. Formalize the queuing process of the BEV e^* in station c_i at time t as follows:

$$p_{c_i}^{*,t} = \arg \min \left\{ T_{p_{c_i}^1}^t, T_{p_{c_i}^2}^t, \dots, T_{p_{c_i}^j}^t \right\} \quad (17)$$

$$t_{wc_i}^{e^*} = T_{p_{c_i}^{*,t}}^t \quad (18)$$

$$T_{p_{c_i}^{*,t}}^t = T_{p_{c_i}^{*,t}}^t + t_{cc_i}^{e^*} \quad (19)$$

$$t_{sc_i}^{e^*} = t_{wc_i}^{e^*} + t_{cc_i}^{e^*} \quad (20)$$

where (17) captures the charger with the minimum RWT in station c_i at time t , which will be occupied by the arrival BEV e^* . Thus, as shown in (18), the waiting time of BEV e^* at the charging station is equal to the RWT of charger $p_{c_i}^{*,t}$. Then, the status of the charging station and BEV would be updated. In (17), the RWT of $p_{c_i}^{*,t}$ charger would be updated by adding the charging time $t_{cc_i}^{e^*}$. The total service time of BEV is calculated by (20).

D. Dynamic Network Loading

The DNL mainly simulates the process of traffic flow transmission on the link of the network, including two parts: link update and flow computation. Considering that the expressway network is normal and well-functioning, there is no traffic flow spillback phenomenon. Qian *et al.* [55] found that the travel time predicted by the point queue model is the same as the kinematic wave (LWR) model's prediction when queues in the downstream links do not grow to block in which a link exits. Hence, the point queue model is used to capture the congestion on the link due to its simplicity and efficiency.

1) Link Update:

$$X_a^t = X_a^{e,t} + X_a^{g,t} \quad \forall a \in A, t \in T \quad (21)$$

$$X_a^{g,t} = X_a^{g,t-1} + (u_a^{g,t} - v_a^{g,t})T/S \quad \forall a \in A, t \in T \quad (22)$$

$$X_a^{e,t} = \begin{cases} X_a^{e,t-1} + (u_a^{e,t} - v_a^{e,t})T/S & a \notin A_c \\ X_a^{e,t-1} + (u_a^{e,t} - v_a^{e,t})T/S + d_a^{t-1} - d_a^t a \in A_c \end{cases} \quad \forall a \in A, t \in T. \quad (23)$$

This part is used to update each link occupancy at each period. As shown in (21), the real-time occupancy of link a is the sum of GV occupancy and BEV occupancy on link a at time t .

Due to links with charging stations, the BEV in charging stations does not affect the network flow. Therefore, we discuss the link update of GVs and BEVs, as shown in (22) and (23), respectively. The links equipped with charging stations or not are the same for GV. When there is no charging station in link a , the link update of BEVs is the same as GV, while, if the link a is equipped with a charging station, the charging BEV, which is serviced in the charging station, is not included in the link a .

2) Flow Computation:

$$\sum_{m \in M} v_a^{m,t+\tau_a^{m,t}} = \frac{\sum_{m \in M} u_a^{m,t}}{1 + (\tau_a^{m,t} - \tau_a^{m,t-1})/(T/S)} \quad \forall a \in A, t \in T \quad (24)$$

$$\sum_{m \in M} v_a^{m,t+\tau_a^{m,t}} = \begin{cases} LC_a & \tau_a^{m,t} > t_a^m \\ \sum_{m \in M} u_a^{m,t}, & \tau_a^{m,t} \leq t_a^m \end{cases} \quad \forall a \in A, t \in T. \quad (25)$$

Equation (24) illustrates the relationship between the outflow rate, the inflow rate, and the link's travel time at each period. According to the point queuing theory, as shown in (25), the outflow rate of the link will be affected by both the inflow rate and the exit capacity of the link.

Meanwhile, the flow propagation needs to satisfy the constraint of node flow conservation. That is, the inflow rate of the node is equal to the outflow rate at each period. Considering the flow of loading and leaving the network, we propose a generalized equation for various types of nodes, including ordinary nodes, source nodes, sink nodes, diverging nodes, and merging nodes

$$\sum_{a \in EE(n)} v_a^{m,t} = \sum_{s \in D} \sum_k f_{ns,k}^{m,t} + \sum_{a \in ES(n)} u_a^{m,t} \quad (26)$$

where $\sum_{s \in D} \sum_k f_{ns,k}^{m,t}$ is the new loading flow of vehicle m on node n at time t .

E. Overall DTA Formulation

The other dynamic simulated system constraints include initialization, OD demand conversation, and nonnegativity, which are shown as follows:

$$X_a^{m,1} = 0, d_a^1 = 0 \quad \forall a \in A, m \in M \quad (27)$$

$$u_a^{m,t} = \sum_{rs} \sum_{k \in K_{rs}} u_{rs,k}^{m,t} \cdot \delta_{rs,k}^a \quad \forall m \in M, a \in A, t \in T \quad (28)$$

$$v_a^{m,t} = \sum_{rs} \sum_{k \in K_{rs}} v_{rs,k}^{m,t} \cdot \delta_{rs,k}^a \quad \forall m \in M, a \in A, t \in T \quad (29)$$

$$\sum_{k \in K_{rs}^m} u_{rs,k}^{m,t} = q_{rs,k}^{m,t} \quad \forall r \in O, s \in D, m \in M, t \in T \quad (30)$$

$$u_a^{m,t} \geq 0, v_a^{m,t} \geq 0, X_a^{m,t} \geq 0, \tau_a^{m,t} \geq 0 \quad \forall a \in A, m \in M, t \in T. \quad (31)$$

As shown in (27), the flow on each link and charging station is zero at the beginning of simulation; (28)–(30) illustrate the basic relationship between each link's inflow rate and outflow rate; and the nonnegativity constraints for inflow rate, outflow rate, flow, and travel time are described as (31).

In this article, the objective function in the lower model is the SDUE, which is shown as (34). When the system approaches the SDUE status each time, no user can improve his/her experienced travel time by unilaterally switching routes [51], [53]. The minimum expected travel costs of BEV/GV on (r, s) , $\mu_{rs}^{e,t}$, and $\mu_{rs}^{g,t}$ are calculated as (32) and (33), respectively. Furthermore, the variational inequality (VI) of DTA is formulated as (34)

$$\mu_{rs}^{e,t} = -\frac{1}{\theta} \ln \left[\sum_{k \in K_{rs}^e} \exp(-\theta C_{e^*}) \right] \quad \forall r \in O, s \in D \quad (32)$$

$$\mu_{rs}^{g,t} = -\frac{1}{\theta} \ln \left[\sum_{k \in K_{rs}^g} \exp(-\theta C_{g^*}) \right] \quad \forall r \in O, s \in D \quad (33)$$

$$\begin{aligned} & \sum_{rs} \sum_{k \in K_{rs}^e} \sum_t \left\{ C_{e^*} \cdot f_{e^-} + \frac{1}{\theta} [\ln(f_{e^-}^\Phi) - \ln(q_{rs}^{e,t})] - \mu_{rs}^{e,t} \right\} \\ & \quad \times (f_{e^*} - f_{e^*}^\Phi) \\ & + \sum_{rs} \sum_{k \in K_{rs}^g} \sum_t \left\{ C_{g^*} \cdot f_{g^-} + \frac{1}{\theta} [\ln(f_{g^-}^\Phi) - \ln(q_{rs}^{g,t})] - \mu_{rs}^{g,t} \right\} \\ & \quad \times (f_{g^*} - f_{g^*}^\Phi) \geq 0 \end{aligned} \quad (34)$$

where the variable with Φ is the solution of the model. Under the Kuhn–Tucker condition of VI, when $f_{rs,k_1}^\Phi > 0$ and $f_{rs,k_2}^\Phi > 0$, the formula is (35), which proves the equivalence between the VI model and the equation of traffic network equilibrium with the mixed flow [see (11) and (15)]. Since the feasible region of the model is composed of linear constraints, and $C_{rs,k}^m(f_{rs,k}^{m,t})$ is the continuous monotone increasing function of

flow $f_{rs,k}^{m,t}$ on route k , the model has a unique solution

$$\left. \begin{aligned} C_{e^*}(f_{e^*}) + \frac{1}{\theta} [\ln(f_{e^*}^\Phi) - \ln(q_{rs}^{e,t})] - \mu_{rs}^{e,t} &= 0 \\ C_{g^*}(f_{g^*}) + \frac{1}{\theta} [\ln(f_{g^*}^\Phi) - \ln(q_{rs}^{g,t})] - \mu_{rs}^{g,t} &= 0 \end{aligned} \right\} \Rightarrow \left\{ \begin{aligned} f_{e^*}^\Phi &= q_{rs}^{e,t} \exp(-\theta C_{e^*}(f_{e^*}) + \theta \mu_{rs}^{e,t}) \\ f_{g^*}^\Phi &= q_{rs}^{g,t} \exp(-\theta C_{g^*}(f_{g^*}) + \theta \mu_{rs}^{g,t}). \end{aligned} \right. \quad (35)$$

V. UPPER MODEL—CHARGING STATION DEPLOYMENT

The expressway charging station deployment model optimizes the layout from two aspects: selecting charging stations from the existing service areas and determining the number of chargers in each charging station. The objectives of the upper model should be constructed from the perspective of BEV drivers and planners, respectively. On the one hand, the construction cost, depending on the number of charging stations and chargers, should be minimized to avoid facility resource waste. It can be formulated as

$$\text{Min } Z_{\text{con}}(\mathbf{y}) = \sum_{i \in \phi} [y_i(\mathbf{y}) \cdot B_1 + p_i(\mathbf{y}) \cdot B_2]. \quad (36)$$

On the other hand, to improve the service level of charging facilities, the total travel cost of BEVs should be as small as possible, namely,

$$\text{Min } Z_{\text{tra}}(\mathbf{y}) = \sum_{t \in T} \sum_{r \in R} \sum_{s \in S} \sum_{k \in K_{rs}^e(\mathbf{y})} f_{rs,k}^{e,t}(\mathbf{y}) \cdot C_{rs,k}^{e,t}(\mathbf{y}). \quad (37)$$

It is obvious that there is a conflict of interest between the two objectives. To overcome this conflict, a weighted linear combination (WLC) method, which is intuitive and widely used way in previous similar studies [11], [56], is introduced in this article. By using this method, two conflict objectives can be converted into one. Since two objectives in this article have the same unit of measurement (i.e., measured by monetary cost), the newly converted objective can also be measured by monetary cost. As shown in (38), the objective function of the upper model is written as minimizing the total objective cost $Z(\mathbf{y})$, which is combined with the weighted construction cost [i.e., $\omega_1 \cdot Z_{\text{con}}(\mathbf{y})$] and the weighted total BEV travel cost [i.e., $\omega_2 \cdot Z_{\text{tra}}(\mathbf{y})$]

$$\min Z(\mathbf{y}) = \omega_1 \cdot Z_{\text{con}}(\mathbf{y}) + \omega_2 \cdot Z_{\text{tra}}(\mathbf{y}). \quad (38)$$

Using $K_{rs}^e(\mathbf{y})$, $f_{rs,k}^{e,t}(\mathbf{y})$, and $C_{rs,k}^{e,t}(\mathbf{y})$ highlights the impact of the infrastructure layout \mathbf{y} on the effective route set, the flow distribution, and the generalized cost of BEVs. The constraints are shown as follows:

$$y_i \in \{0, 1\} \quad \forall i \in \phi \quad (39)$$

$$y_i \cdot p_{\min} \leq p_i \leq y_i \cdot p_{\max} \quad \forall i \in \phi \quad (40)$$

$$Z_{\text{con}}(\mathbf{y}) \leq B^* \quad (41)$$

$$(\bar{\mathbf{v}}, \bar{\mathbf{f}}) = \arg \min_{\mathbf{v}, \mathbf{f}} \sum_{m \in M} \sum_{t \in T} \sum_{r \in R} \sum_{s \in S} \sum_{k \in K_m^g(\mathbf{y})} f_{rs,k}^{m,t}(\mathbf{y}) \cdot C_{rs,k}^{m,t}(\mathbf{y}). \quad (42)$$

Equation (39) means that one charging station can be built at one location at the most. Equation (40) is the quantity constraint of chargers. Meanwhile, considering the limited

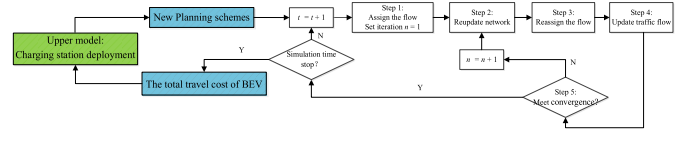


Fig. 5. Algorithm of MSA.

finances, the construction cost constraint is proposed as (41). Equation (42) states that the DTA model simulates the traffic flow distribution and the operational status of each charging station at each period.

VI. SOLUTION ALGORITHM

The proposed bilevel optimization deployment model is hard to solve due to the problem's inherent complexity. The heuristic algorithm is a useful and effective method for NP-hard problems [27]. As one of the heuristic algorithms, GA shows good performance in solving discrete problems and evolves the population to globally optimal solutions based on natural evolutionism [57]. It has been applied to solve the deployment problems [10], [13], [28], [58].

For the SDUE problem, it is very hard to calculate the descent direction and the iteration step. Given the maximum MSA iteration number and the tolerance value, the MSA method can converge effectively and obtain equilibrium solutions accurately. It is an effective solution algorithm for traffic flow assignment problems in large-scale networks and is widely used [59]–[61]. Here, the flow distribution adopts a stochastic flow assignment method; the iteration step is given as $1/n$, where n is the iteration number; and the descent direction is the difference between the additional traffic volume at iteration n and the traffic volume at last iteration $n-1$.

Therefore, the MSA and GA are adopted to solve the assignment model and the optimization model, respectively. The algorithm relationship between the upper model and the lower model is shown in the Appendix. Based on the charging stations' layouts origin from the upper model, the stochastic UE results are obtained by the MSA. Then, the total travel cost of BEVs and the construction cost are inputted into the upper model to calculate the fitness of planning schemes. Finally, the GA process optimizes the new planning scheme and outputs it into the lower model for the next iteration. The optimal planning scheme is obtained at the end of the GA iteration.

A. Method of Successive Weight Averages for DTA

The basic idea of MSA is to continuously adjust the flow distribution of each link, and then, the system gradually approaches the balanced distribution. The algorithm of MSA is shown in Fig 5. It is noted that, considering the computational load, this lower simulation assumes that drivers choose the route when entering the network and do not change the route during the trip.

The specific steps are given as follows.

Step 0: Based on the deployment of charging stations, the effective route sets of BEV (K_{rs}^e) and GV (K_{rs}^g) are constructed by (1) and (2).

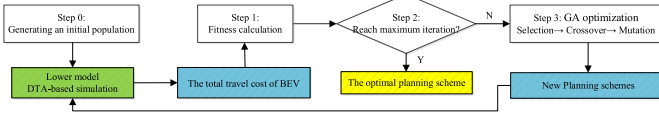


Fig. 6. Algorithm of GA.

For $t \in T$:

Step 1: Based on the flow on each link and the status of each charging station at the end of the last time $t-1$, calculate the generalized travel cost $H_a^{m,t,(0)}$, the choosing probability $P_{rs,k}^{m,t,(0)}$, and the queue length $q_a^{t,(0)}$. Then, the status of each charging station $\{T_{p_{ci}}^{t,(1)}\}$ and the flow on each route $\{X_a^{t,(1)}\}$ are updated by (17)–(17) and (21)–(23), respectively. Set the iteration $n = 1$.

Step 2: Recalculate the generalized travel cost $H_a^{m,t,(n)}$, the choosing probability $P_{rs,k}^{m,t,(n)}$, and the queue length $q_a^{t,(n)}$ according to the flow distribution $\{X_a^{t,(n)}\}$ and the status of the charging station $\{T_{p_{ci}}^{t,(n)}\}$ at the last iteration. It is noted that the link time of virtual roads for charging stations is updated by the minimum RWT of charging stations at the last iteration.

Step 3: Based on results in step 2, reassign the BEV flow and the GV flow, respectively, in the network. Then, the auxiliary flow of each link is calculated as $\{Y_a^{t,(n)}\}$.

Step 4: Update the traffic flow as follows:

$$X_a^{t,(n+1)} = X_a^{t,(n)} + \lambda^{(n)} \cdot (Y_a^{t,(n)} - X_a^{t,(n)}) \quad (43)$$

$$\lambda^{(n)} = n / (1 + 2 + 3 + \dots + n). \quad (44)$$

Step 5 (Convergence Test): Calculate the convergence by the following relative gap function:

$$\text{gap} = \sqrt{\sum_{a \in A} (X_a^{t,(n+1)} - X_a^{t,(n)})^2} / \left(\sum_{a \in A} (X_a^{t,(n)}) \right). \quad (45)$$

If the *gap* is less than the predetermined tolerance value ε , the algorithm ends in this interval and outputs the total BEV travel cost to the upper model. Otherwise, set $n = n+1$, and go to step 2.

B. Genetic Algorithm for Optimization Model

The optimization process of the GA algorithm is depicted in Fig 6. We use the binary real-coded method to build the chromosome illustrating the deployment of charging stations. As shown in Fig. 7, the first line shows the binary variable about the construction situation of charging stations, where 1 means that a charging station is built in this area, otherwise 0. The second line shows the number of chargers in each area. If the one charging station is built in this area, the charger should be built in the range of $[p_{\min}, p_{\max}]$.

The fitness function of GA, denoting the quality of each chromosome, is the reciprocal of the sum of the construction cost and the total BEV travel cost. The selection process adopts the roulette wheel method, and the usual linear crossover and linear mutation are applied to create a new chromosome and avoid the local optimum. It should be noted that all the new planning schemes satisfy the related requirements after the

Area 1	Area 2	Area	Area 22	Area 23
0	1	...	0	1
0	7	...	0	5

Fig. 7. Coding process of two variables.

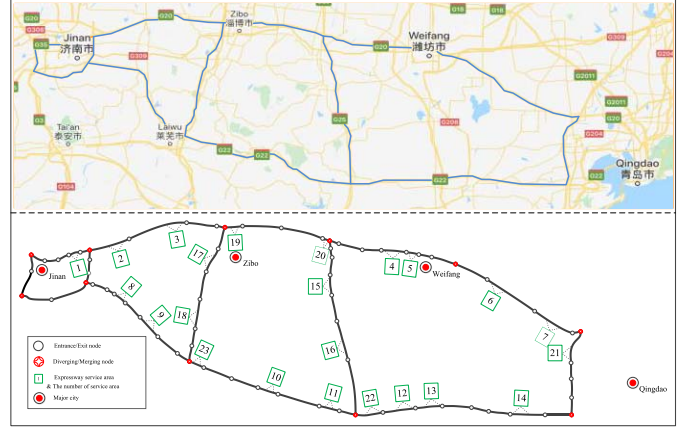


Fig. 8. Topology network of the expressway in Shandong province.

above process. Based on the proposed illustrations, the steps of GA are shown as follows.

Step 0 (Initialization): Set the population size, maximum iterations, crossover probability, and mutation probability, and generate an initial population.

Step 1: Calculate the fitness of each planning scheme by the lower model, and find the optimal scheme with the best fitness function.

Step 2: Judge the criteria of termination. If the iteration reaches the maximum number, the bilevel programming algorithm terminates. Otherwise, the optimal process continues.

Step 3: Through selection, crossover, and mutation in order, the new population for the next iteration is generated.

VII. CASE STUDY

A. Description of Case Network

To evaluate the proposed model and algorithm, a real case network in the Shandong province of China is tested in this section. It is a part of the whole expressway network of Shandong province, which includes seven national highways and one provincial highway. The total length of the network is 1137.3 km. The topological graph of the network is shown in Fig. 8, which consists of 66 entrance/exit nodes, 864 OD pairs, 69 road sections, and 23 service areas.

In this case, a whole day traffic flow from 0:00 A.M. to 24:00 A.M. on October 19, 2012, is considered. The total traffic flow is 91 057 pcus. All OD flows are given every interval time, which is set as 15 min. Namely, 96 intervals are included in the case. The percentage of BEV flow is assumed to be 40%. The temporal distribution feature of three flows

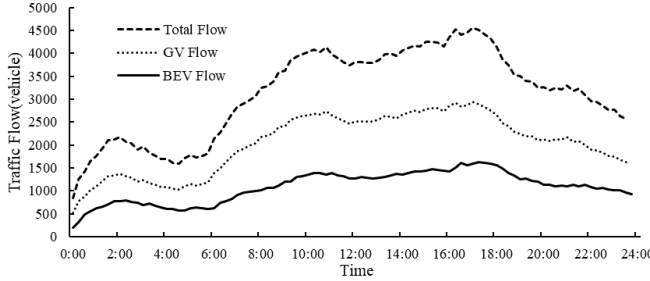


Fig. 9. Real-time distribution of traffic flow.

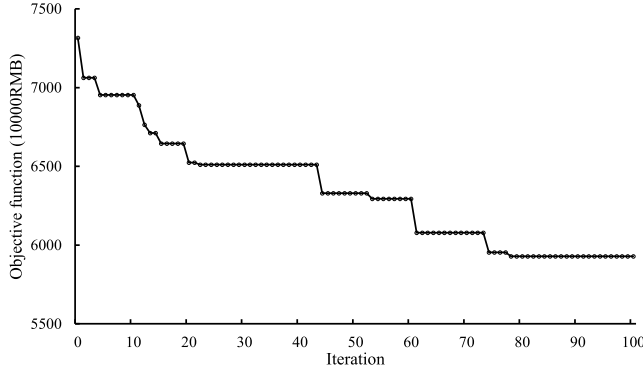


Fig. 10. Optimization process of GA.

(i.e., total flow, GV flow, and BEV flow) in the network is shown in Fig. 9. From 8:00 to 22:00, the total flow is over 3000 vehicles in every interval time. Two peak periods, during which the total flow exceeds 4000 vehicles in every interval, existed between 9:00~11:00 and 14:00~18:00, respectively.

The construction costs of charging station and charger are taken as 2050000 RMB, respectively. The minimum and maximum charger numbers in one charging station are set as 3 and 10, respectively. Other parameters are set as follows: $S_1 = 20\%$, $S_1 = 40\%$, $S_n^{e*,0} = 100\%$, $U = 380$ V, $a^e = a^g = 1$, $\alpha^{rs,e} = \gamma^{rs,e} = \alpha^{rs,g} = 34$ RMB·h $^{-1}$, $\beta^{rs,e} = 0.488$ RMB·km $^{-1}$, $\beta^{rs,g} = 1.0$ RMB·km $^{-1}$, $Q = 40$ A·h, $\theta = 1$, $\varepsilon = 0.05$, $\omega_1 = \omega_2 = 0.5$, and $B^* = 25$ million RMB.

B. Results

1) *Best-Found Result*: The proposed model is tested on a personal computer with Intel Core i7-8650U 1.90 GHz and 16-GB RAM. The population size, the maximum number of iterations, crossover probability, and mutation probability are set to 30, 100, 0.8, and 0.6, respectively. Fig. 10 illustrates the optimization process of GA. The optimal solution is obtained after 78 iterations. The execution time is about 48 h.

The best-found solution is given in Table I. The corresponding deploying scheme is depicted in Fig. 11, in which different colors display the number of chargers (the darker the color is, the more the chargers are). As shown in Table I, six expressway service areas (namely, areas with the number of 3, 4, 13, 16, 18, and 23) are selected to build the charging station, with a total of 40 chargers.

2) *Analysis of the LOS of Charging Station*: Four indexes were used to evaluate the LOS of the charging station. Results

TABLE I
BEST-FOUND AVAILABLE SOLUTION

The number of service area	1	2	3	4	5	6	7	8	9	1	1	1	1	1	1	1	1	2	2	2	
Selected as charging station or not	0	1	1	0	0	0	0	0	0	1	0	0	1	0	1	0	0	0	1	2	3
Number of chargers in selected service area	-	5	6	-	-	-	6	-	-	8	-	6	-	-	9	-	-	-	-	-	-

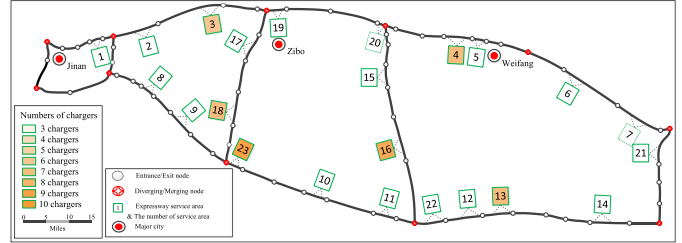


Fig. 11. Spatial distribution of charging facilities in the best-found solution.

TABLE II
PERFORMANCE OF EACH CHARGING STATION

Indicators	The number of service area with charging stations					The system	
	3	4	13	16	18		
The number of BEVs with charging event	351	273	200	276	53	579	1732
Avg. charging time (min)	15.58	20.51	16.42	18.66	20.81	15.05	16.93
Avg. waiting time (min)	15.72	7.67	0.87	1.01	0.26	15.31	9.78
Avg. value of status U_1	1.50	0.95	0.41	0.43	0.10	1.46	0.82
Avg. utilization rate U_2	0.76	0.65	0.38	0.45	0.13	0.67	0.51

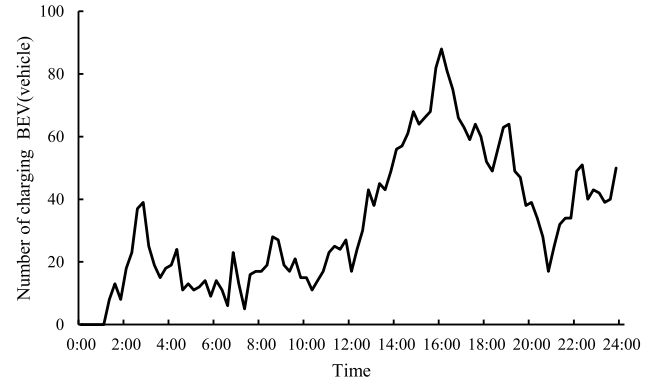


Fig. 12. Real-time charging demand.

of each station and the whole system are shown in Table II. Among the four indexes, two were related to BEVs charging in stations, namely, the average charging time and the average waiting time. The other two were related to stations directly, namely, the average value of status and the average utilization rate.

The average value of status, U_1 , indicates the average state of a charging station at the end of each time interval. It is the ratio of the number of charging and waiting BEVs to the number of chargers. When $U_1 = 1$, it means that all chargers are used, and no BEV is waiting for charging. When $U_1 < 1$,

it means that a proportion of chargers are idle. The lower value the U_1 is, the more idle chargers exist. When $U_1 > 1$, it means that the number of BEVs waiting for charging is about $(U_1 - 1)$ times as much as the charger number. U_1 can be calculated by

$$U_1 = \sum_{t \in T} (d_{c_i}^t / p_{c_i}) / S' \quad (46)$$

where $d_{c_i}^t$ represents the number of BEVs charging/waiting at charging station i at time t ; p_{c_i} is the sum of chargers at charging station i ; and S' is the number of time parts.

The average utilization rate, U_2 , indicates the usage rate of a charging station from the respective of time. It is the ratio of the total working time to a whole day time. It is obvious that all stations are supposed to have a high value. U_2 can be calculated by

$$U_2 = \sum_{e^*} t_{cc_i}^{e^*} / p_{c_i} \cdot T \quad (47)$$

where $\sum_{e^*} t_{cc_i}^{e^*}$ is the sum of charging time of all BEVs at charging station i .

As shown in Table II, the whole system's average charging time and waiting time are 16.93 and 9.78 min, respectively. U_1 and U_2 for the whole system are 0.82 and 0.51, respectively, indicating that the utilization rate of the whole system is relatively acceptable. Furthermore, the No.3, No.4, and No.23 service areas attract more BEVs and cause a longer queue. As seen in Fig. 11, service areas 3, 4, and 23 are located at the two important routes between Jinan city and Qingdao city. These two routes undertake the primary travel demand and energy demand. Therefore, more chargers should prioritize adding in service areas 3, 4, and 23 to alleviate the working load during peak hours if with a higher investment budget.

3) *Analysis of the Time-Variant State of Charging Stations:* By introducing time coordinates, the time-variant feature of traffic flow can be captured accurately. The real-time operating status of charging facilities under the optimal layout is analyzed as follows. The time-variant characteristics of charging demand (that is, the total number of BEVs) and facilities' working status (the minimum waiting time, that is, the minimum remaining working time of chargers) in each charging station are shown in Figs. 12 and 13, respectively.

As shown in Figs. 12 and 13, the charging demand is less than 30 vehicles, and the minimum waiting time of each charging station is less than 20 min in 0:00~12:00 and 20:00~22:00, illustrating that the whole optimal system is under a stable and low load in the current periods. In the period of 14:00~19:00, the demand reaches more than 50 vehicles, and the minimum waiting time in stations 3 and 23 is more than 30 min, illustrating that the system with 40 chargers is in a high-load state. It is observed that the temporal distributions of charging demand and minimum waiting time are similar to that of traffic flow, with a certain time lag.

C. Algorithm Efficiency

The algorithm performance of GA is compared with the simulated annealing (SA) and the particle swarm optimization (PSO). Based on the thermodynamics of the metal cooling process, SA is a heuristic method to find a global optimum

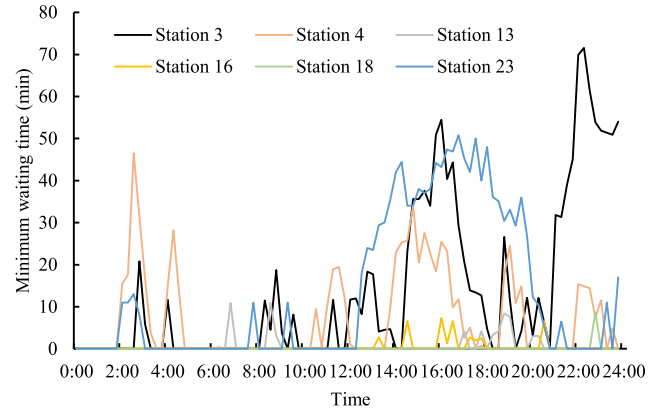


Fig. 13. Real-time minimum waiting time.

TABLE III
RESULTS IN DIFFERENT ALGORITHMS

	GA	SA	PSO
The total objective cost (10^7 RMB)	2.96 (0%)	3.00 (+1.16%)	3.06 (+3.24%)
CPU time (hour)	40 (0%)	51 (+21%)	42 (+5%)

solution [62]. In the SA algorithm, the initial temperature, the final temperature, and the coefficient controlling the cooling schedule are set as 100, 0.01, and 0.9, respectively. The new feasible solution is randomly generated from three neighboring solutions at a particular temperature, and the iteration is 50. By the cognition of themself part and the whole social part, the particles are evolved and found the optimal solution through the PSO algorithm [63]. The parameters in the PSO algorithm are set as follows: the population size is 30, the iteration is 100, two study factors are 2.0, and the inertial factor following linear decreasing weight (LDW) strategy ranges from 0.4 to 0.8.

The detailed performances of the three algorithms are shown in Table III. Compared with SA and PSO, GA finds the best solution with the shortest execution time. The total objective cost of the optimal solution obtained by SA and PSO is 1.16% and 3.24% higher than GA. The execution times of SA and PSO are 21% and 5% longer than GA, respectively. The GA algorithm is demonstrated to be effective and efficient in solving the proposed deployment problem.

D. Comparing With STA-Based Models

As mentioned in Section II, the STA-based facility location model has been widely used for charging station deployment. To verify the validity and necessity of the proposed bilevel model, we compare the optimal layouts of the DTA-based deployment model and the STA-based deployment model with the actual layout. In China, the construction of fast charging stations on the expressway is in the initial stage. In order to occupy the market share, operators pay more attention to the construction of charging stations, while the average number of chargers is only 4 [3]. Therefore, the actual layout in this article refers to each service area is equipped with four chargers, which can be seen in Table IV.

TABLE IV
LAYOUTS' COMPARISON

layouts	Service area ID													Sum ¹	Sum ²								
	1	2	3	4	5	6	7	8	9	10	11	12	13	14	15	16	17	18	19	20	21	22	23
Current	4	4	4	4	4	4	4	4	4	4	4	4	4	4	4	4	4	4	4	4	4	23	92
STA	-	4	7	-	8	-	3	-	8	-	-	-	6	-	-	3	-	6	-	8	-	45	
DTA	-	-	5	6	-	-	-	-	-	6	-	8	-	6	-	-	-	9	6	-	-	40	

¹ The sum of charging stations

² The sum of chargers

TABLE V
LOS COMPARISON AMONG DIFFERENT MODELS

Indicators	Layouts		
	Current	STA	DTA
Avg. charging time (min)	17.0(0%)	17.4(+2.4%)	16.9(+0.6%)
Avg. waiting time (min)	124.0(0%)	93.4(-24.7%)	9.8(-92.1%)
Avg. value of status U_1	4.60(0%)	1.62(-64.8%)	0.82(-82.2%)
Avg. utilization rate U_2	0.68(0%)	0.34(-50%)	0.51(-25%)
Equilibrium $E(U_c)$	2.06(0%)	0.89(+56.8%)	0.42(+79.6%)

The charging service process is analyzed by M/M/1 queue model in the STA-based deployment model. The waiting time function adopts the following form [20], [64]:

$$t_{wc_i} = t_{wc_i}^0 \cdot \left[1 + \frac{u_{ci}}{C_{ci}} + \frac{u_{ci}^2}{C_{ci}^2} \right] \quad (48)$$

where $t_{wc_i}^0$ is the free-flow waiting time at the charging station c_i , which is set as 2 min; u_{ci} is the number of charging events. C_{ci} represents the service capacity of the charging station c_i , which depends on the chargers' quantity and is assumed that one charger can service four vehicles in 1 h.

Meanwhile, $E(U_c)$ is introduced to depict the spatial equilibrium of utilization rate, which is shown as follows:

$$E(U_c) = \frac{S(U_c)}{B(U_c)} \quad (49)$$

where U_c is the set of charging stations' utilization U_2 . $S(U_c)$ and $B(U_c)$ are the standard deviation and the average value of U_c , respectively. The calculation form of (49) expresses the set equilibrium of U_c , per unit U_c . $E(U_c)$ evaluates the network's spatial equilibrium of each charging station's utilization. The larger the $E(U_c)$, the more disequilibrium the facilities' utilization.

The optimal layouts are illustrated in Table IV. The construction scale of charging infrastructures under the DTA-based layout is significantly less than the current layout and the STA-based layout.

The corresponding LOS of each layout is shown in Table V. The average charging time of the current layout is minimal, only 16.7 min. It is because BEV drivers can charge at any service area on the network with many charging stations. With a smaller number but more reasonable deploying of charging stations, the average charging time and the construction scale of the DTA-based layout are less than the STA-based. Compared with the current layout, the average waiting time and the average value of status U_1 of the DTA-based layout are reduced

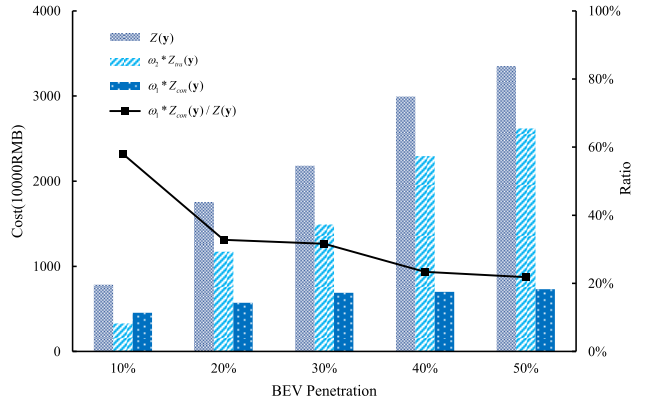


Fig. 14. Variation of different costs and the proportion of construction cost in various BEV penetrations.

by 84.2% and 54.2%, far less than the STA-based layout. The facility utilization U_2 has improved to 0.51 in the DTA-based layout, indicating that the daily working load of the charging system is most stable compared with the other two layouts. Meanwhile, $E(U_c)$ of the DTA-based layout is 0.42, which illustrates that a large but unreasonable infrastructure deployment may cause charging facilities with a lower utilization rate and a spatial disequilibrium of utilization rate. Also, it may decline the whole system's LOS. Therefore, the DTA-based deployment model is proven to be an effective and feasible method for public charging stations deployment planning on the expressway network.

E. Sensitivity Analysis of Percentage of BEV Flow

With the development of battery technology and the improvement of people's recognition/acceptance, the market share of BEVs will gradually increase. Based on five scenarios, this section focuses on the dynamic optimization layouts in various BEV penetrations. The percentage of BEV flow is assumed to be 10%, 20%, 30%, 40%, and 50%, respectively.

With the increase in BEV flow's percentage, the overall developing trends of $Z(y)$ (the total objective cost), $\omega_1 * Z_{con}(y)$ (the weighted construction cost), and $\omega_2 * Z_{tra}(y)$ (the weighted BEV travel cost) increase (in Fig. 14). $\omega_1 * Z_{con}(y)$ of charging facilities increases relatively slowly, and its proportion in the total objective cost $\omega_1 * Z_{con}(y)/Z(y)$ gradually decreases from the initial 58% to 20%. In the preliminary of charging station deployment, $\omega_1 * Z_{con}(y)/Z(y)$ is up to 58%. The proportion gradually levels off and eventually reaches 20% with the increase in charging stations' scale. Through the lifecycle management of charging facilities, charging facility operators try to provide a high and stable LOS and achieve industry profits.

Then, we analyze the system's operating status in various BEV flow penetrations, as shown in Table VI. Regarding the current layouts, the utilization of charging facilities and the congestion degree in the charging station are greater

TABLE VI

COMPARISON OF CHARGING STATIONS UNDER DTA-BASED LAYOUTS AND CURRENT LAYOUTS

Indicators	The percentage of BEV flow (%)				
	10	20	30	40	50
The operating status of DTA-based layout					
Avg. charging time (min)	16.2	18.0	17.5	16.9	16.9
Avg. waiting time (min)	0.0	2.2	4.3	9.8	7.7
Avg. value of status U_1	0.10	0.41	0.52	0.82	0.66
Avg. utilization rate U_2	0.10	0.32	0.38	0.51	0.44
Equilibrium $E(U_c)$	0.71	0.52	0.55	0.42	0.42
The operating status of current layout					
Avg. charging time (min)	16.0	16.6	16.7	17.0	17.0
Avg. waiting time (min)	4.5	23.4	57.0	124.0	138.2
Avg. value of status U_1	0.14	0.80	1.79	4.60	5.71
Avg. utilization rate U_2	0.11	0.34	0.46	0.68	0.72
Equilibrium $E(U_c)$	4.32	2.68	2.40	2.06	1.90

than the optimal results. When the BEV percentage is more than 20%, the current layouts' average waiting time and the average value of status U_1 are far beyond the tolerable range. Currently, most charging events are concentrated in several charging stations, while the other charging stations are under low load or not working for a long time [65]. Although it is constructed with 23 charging stations and 92 chargers on the expressway, there still exists a mismatch between charging supply and charging demand.

In the DTA-based layouts, the average charging time and the average waiting time of BEVs with charging events are distributed in 16~18 and 0~10 min, respectively. U_1 and U_2 are distributed in 0.10~0.82 and 0.10~0.51, respectively. As shown in the comparison of $E(U_c)$, the network working load under the DTA-based layouts is more equilibrium. With the increase in BEV penetrations, the network's spatial distribution of working load is more equilibrium, decreasing from 0.71 to 0.42. In conclusion, the DTA-based layout provides a high LOS for BEV users, and the whole charging facilities are under a reasonable and equilibrium operating load.

The optimal schemes are given in Table VII and depicted in Fig. 15. As illustrated in Table VII, the sum of charging facilities increases monotonously with the increase in BEV flow. As BEV penetration increases from 10% to 30%, the number of charging stations increases from 4 to 6 and the number of chargers from 22 to 26. With the further increase in the BEV penetration, the capacity of charging stations increases from 36 to 53, but the number of charging stations remains the same. In the preliminary planning (BEV penetration lower than 30%), planners should focus on the coverage of charging facilities and construct more charging stations to expand the travel range of BEVs. With the further development of BEVs, planners should pay more attention to the LOS of charging facilities and improve the charging station's capacity to guarantee BEV travel satisfaction.

Meanwhile, there is an apparent inheritance and development trend between different optimal plans. In various layouts, No.3, No.4, No.13, No.16, No.18, and No. 23 are selected as charging stations more than three times, and the corresponding charger's quantity increases with the increase in BEV penetrations. In different developing stages, the new

TABLE VII

OPTIMAL SOLUTION OF CHARGING STATIONS AND CHARGERS IN VARIOUS PERCENTAGES OF THE BEV FLOW

Percentage of BEV flow	Service area ID													Sum ¹	Sum ²		
	1	2	3	4	5	6	7	8	9	10	11	12	13	14			
10%	-	-	6	8	-	-	-	-	-	5	-	-	-	-	3	4	22
20%	-	-	3	8	-	-	-	8	-	7	-	-	3	-	-	5	29
30%	-	-	5	3	-	-	-	10	-	5	-	6	7	-	-	6	36
40%	-	-	5	6	-	-	-	6	-	8	-	6	-	-	9	6	40
50%	-	-	9	9	-	-	-	6	-	9	-	10	-	-	106	53	

¹ The sum of charging stations

² The sum of chargers

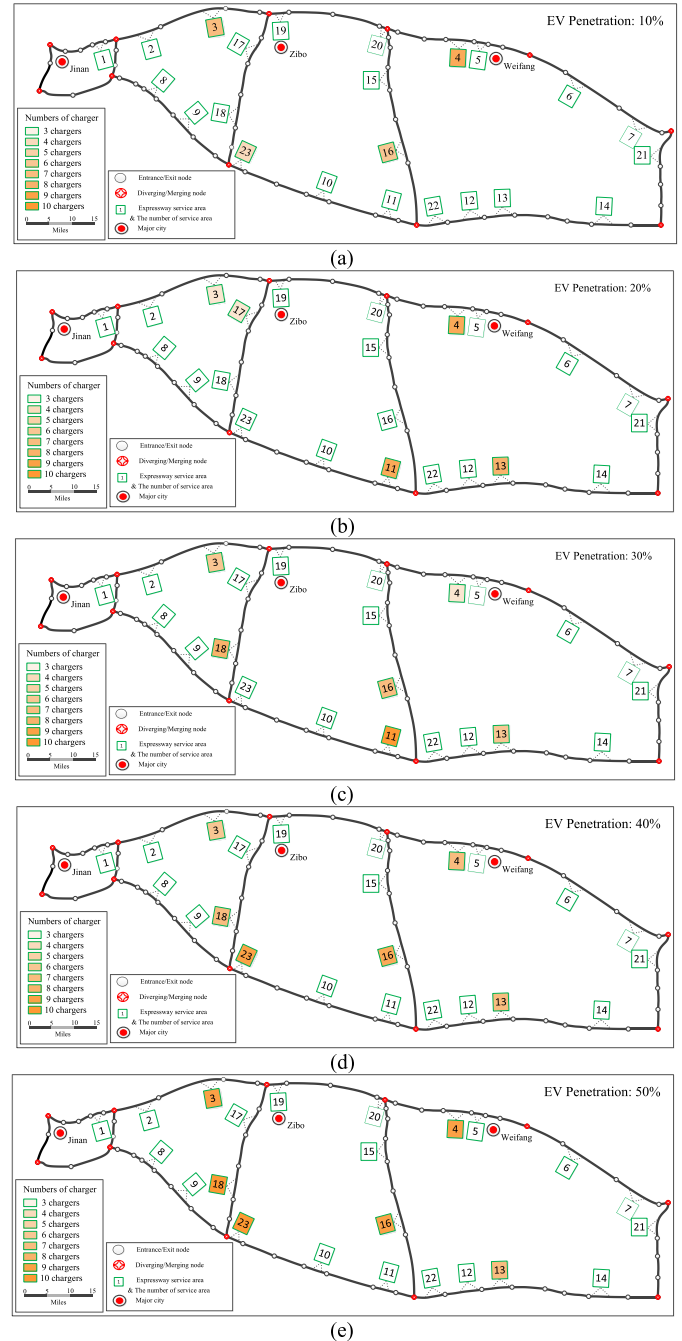


Fig. 15. Spatial distribution of charging facilities in various percentages of the BEV flow. (a) 10% of BEV flow. (b) 20% of BEV flow. (c) 30% of BEV flow. (d) 40% of BEV flow. (e) 50% of BEV flow.

chargers should be constructed in the existing charging stations to satisfy BEV drivers' travel and charging willingness, and save the construction cost of the new charging station.

In various planning strategies, the charging facilities are mainly constructed in the middle of the expressway network, which is No.3, No.4, No.11, No.13, No.16~No.18, and No.23 service areas. Meanwhile, 15 service areas are never selected to build charging stations in the five scenarios. In this expressway network, the traffic flow between Jinan city and Qingdao city accounts for the largest proportion, and the distance is the longest. Thus, the charging stations are not planned in service areas adjacent to the cities (No.1, No.2, No.8, and No.9 adjacent to Jinan city; No.6, No.7, No.14, and No.21 adjacent to Qingdao city). In conclusion, the geographical location of the existing service area, the OD distribution of intercity travel, and the penetration scale of BEV flow are the key factors in the charging station's deployment on the expressway network.

F. Sensitivity Analysis of Objective Weights

The impact of objective weights on the optimal layout and the charging system's LOS is analyzed in this section. As seen in (38), ω_1 and ω_2 are the weights to the construction cost and the total travel cost of BEV in the objective function of the upper model. The sensitivity analysis is conducted with nine scenarios. The construction scale and operating status under various scenarios are shown in Fig. 16. The changes of the two costs are shown in Fig. 16(a), and the corresponding conclusions are shown as follows.

- 1) Continuously increasing BEV's travel cost weight will lead to a continuous increase in construction investment costs. With the increase in ω_2 , the construction scale of charging infrastructures expands, the system's LOS increases (i.e., the average waiting time decreases). As shown in Fig. 16(b), the numbers of stations and chargers increase from 5 to 8 and 24 to 69, respectively, when BEV travel cost weight ω_2 increases from 0.1 to 0.9. The average waiting time decreases from 30.71 to 5.90 min.
- 2) With the increase in ω_2 , the improvement effect of LOS is steadily weakening, and the charging stations are more wasteful. As shown in Fig. 16(c), the average waiting time decreases rapidly from 30.71 to 9.80 min when ω_2 increases from 0.1 to 0.5. With the further increase in ω_2 , the decreasing rate of the average waiting time gradually decreases. In scenario 9, the average value of status (U_1) of the whole system is 0.25, which means that about 75% of chargers are idle.
- 3) The expansion of the charging infrastructure's scale will attract more charging demands. As shown in Fig. 16(d), the number of charging events increases from 1175 to 2041, when ω_2 increases from 0.1 to 0.9. This phenomenon implies that a high level of charging service can encourage the usage of BEVs. Therefore, in the contemporary era of greatly promoting BEV markets, a little bit high value of ω_2 is suggested.

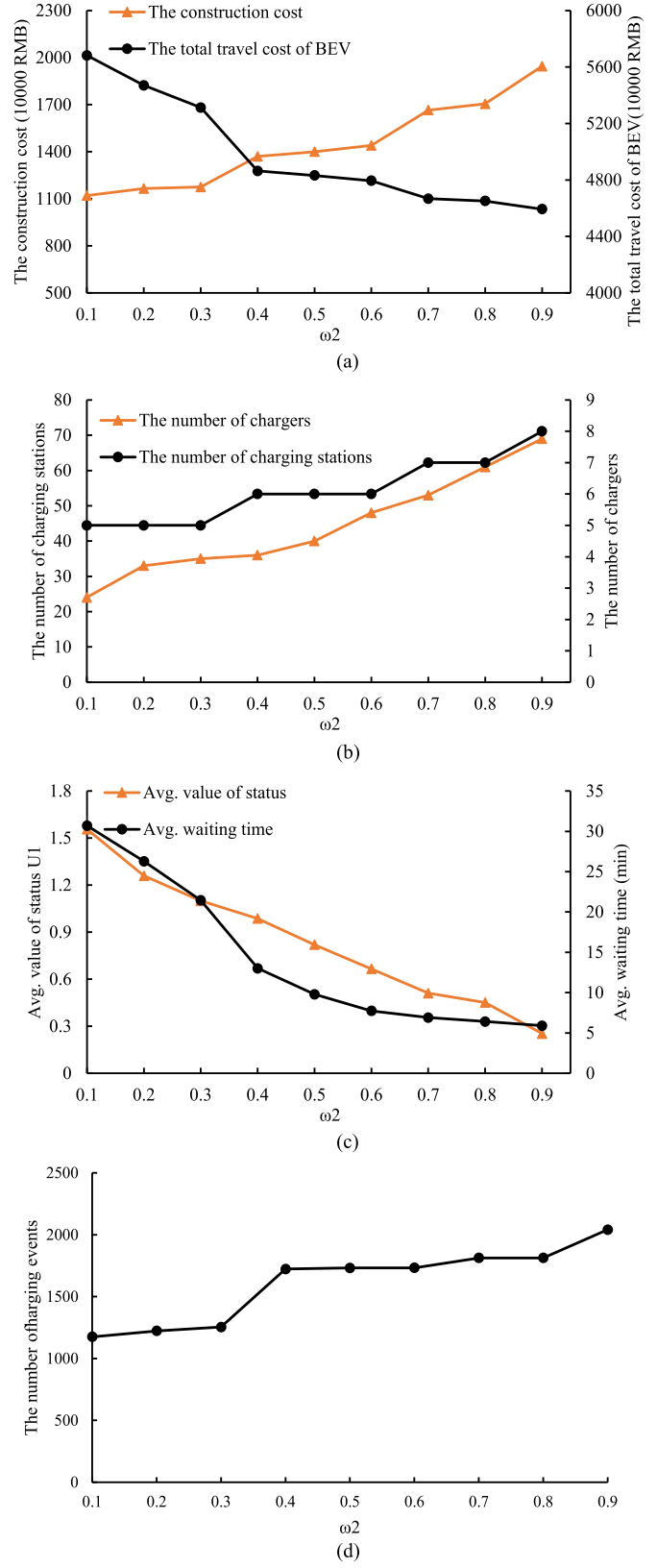


Fig. 16. Performance of best solution in various objective weights. (a) Change of the construction cost and the total travel cost of BEV. (b) Change of the number of charging stations and the number of chargers. (c) Change of the average value of status U_1 and the average waiting time. (d) Change of the number of charging events.

Algorithm 1 Pseudocode of GA Incorporating the Method of Successive Averages

Step 1: (Initialization)

Step 1.1: (Parameter setting) Set population size (P), maximum iterations (M), crossover probability (P_c), and mutation probability (P_m). Set the GA iteration $m = 1$.

Step 1.2: (Generating an initial population)

Do While $p <= P$

Chromosome encoding. The first line the construction situation of charging stations (y_i), the second line shows the number of chargers in each area(p_i).

$p = p + 1$

End Do //p

Return population set P^1

Step 2: (Iterative computation)

Set max DTA iteration (N), tolerance value (ε)

Do While $m <= M$:

For layout y in P^m

Step 2.1: (DTA simulation)

For time $t = t_0$ to T

Set current DTA iteration $n = 1$ and

gap = a big value

Assign and update the traffic flow $\{X_a^{t,(1)}\}$

Do While $gap <= \varepsilon$ or $n > N$:

Update the traffic network $H_a^{m,t,(n)}, P_{rs,k}^{m,t,(n)}, q_a^{t,(n)}$

Calculate the auxiliary flow $\{Y_d^{t,(n)}\}$

Update the traffic flow $\{X_a^{t,(n+1)}\}$

Calculate the convergence gap

$n = n + 1$

End Do //gap, n

End for //t

Return BEV travel cost $Z_{tra}(y)$

End for //y

Step 2.1: (GA optimization)

Calculate the fitness $fit(y)$

Optimize Population by Selection, Crossover,

Mutation P^m

End Do //m

Return best solution p_{best}

VIII. CONCLUSION AND FUTURE RESEARCH

This article aims at deploying the charging stations on expressway networks with the mixed flow of GVs and BEVs. A bilevel model is proposed, including the charging station deployment model and multiclass DTA satisfying the SDUE principle. A virtual edge whose length is determined by the charging service time at each charging station is added to the network to satisfy the FIFO principle. The BEV route choice model considering the travel time, charging time, waiting time, and energy consumption is proposed according to the dynamic status of networks and charging facilities. Thus, it can accurately simulate the travel and charging processes to realize the real-time monitoring of the charging system's working status.

A GA incorporating MSA is proposed to solve the bilevel model. The proposed model and algorithm are tested in an

actual expressway of Shandong province in China. The results show that the proposed algorithm can effectively obtain a deploying scheme for public charging stations on the expressway network with the consideration of dynamic charging demand. It is suggested to give priority to the construction of charging stations in service areas 3, 4, and 23. The performances of the proposed model and algorithm are better than similar previous studies. Compared with SA and POS, the proposed GA method can obtain the best solution with the shortest CPU times. Compared with the STA-based model and the current equalizing deploying strategy, the proposed DTA-based model can provide the best solution with the fewest chargers but the highest LOS. It also implies that the deploying strategy for public charging stations should meet demand adequately, instead of pursuing equality.

Furthermore, considering different planning stages, sensitivity analyses of BEV penetrations and objective weights are provided. The results indicate that, in the preliminary planning, planners should focus on the construction of charging stations to expand the service coverage and expand BEV's travel range. Then, with further development, planners should improve the charging station's capacity to improve BEV's travel satisfaction. A high level of charging service can encourage the usage of BEVs. In the contemporary era of greatly promoting BEV markets, a little bit high value of ω_2 is suggested.

As further extended, more specific travel behavior of BEVs can be considered in this model. It seems useful and instructive for government to research the dynamic layouts of charging stations considering the construction time sequence. Besides, it is better to consider the uncertainties of the traffic situation on different days.

APPENDIX

See Algorithm 1.

ACKNOWLEDGMENT

The authors would like to thank the editor and four reviewers for their helpful suggestions.

REFERENCES

- [1] The Ministry of Public Security of the People's Republic of China. *In the First Quarter of 2021, 9.66 Million New Motor Vehicles Were Registered*. Accessed: Apr. 6, 2021. [Online]. Available: <https://www.mps.gov.cn/n2254314/n6409334/c7829324/content.html>
- [2] The People's Republic of China. *New Energy Vehicle Industry Development Plan (2021-2035)*. Accessed: Nov. 2, 2020. [Online]. Available: http://www.gov.cn/zhengce/content/2020-11/02/content_5556716.htm
- [3] MOT (Ministry of Transport of the People's Republic of China). *By the End of 2018, About 7,500 Charging Piles Had Been Built on Expressways*. Accessed: Oct. 24, 2019. [Online]. Available: https://www.sohu.com/a/349243510_362042
- [4] MOT (Ministry of Transport of the People's Republic of China), *The 14th Five-Year Development Plan for the Integrated Transport Services*, 2021.
- [5] NEA (National Energy Administration). *Annual Report on the Development of China's Charging Infrastructure 2017-2018 Edition*. Accessed: Jul. 15, 2018. [Online]. Available: http://zfxgk.nea.gov.cn/auto84/201808/t20180808_3223.html
- [6] X.-H. Sun, T. Yamamoto, and T. Morikawa, "Fast-charging station choice behavior among battery electric vehicle users," *Transp. Res. D, Trans. Environ.*, vol. 46, pp. 26–39, Jul. 2016.

- [7] K. Chaudhari, N. K. Kandasamy, A. Krishnan, A. Ukil, and H. B. Gooi, "Agent-based aggregated behavior modeling for electric vehicle charging load," *IEEE Trans. Ind. Informat.*, vol. 15, no. 2, pp. 856–868, Feb. 2019.
- [8] L. Pan, E. Yao, and D. MacKenzie, "Modeling EV charging choice considering risk attitudes and attribute non-attendance," *Transp. Res. C, Emerg. Technol.*, vol. 102, pp. 60–72, May 2019.
- [9] O. Teichert, F. Chang, A. Ongel, and M. Lienkamp, "Joint optimization of vehicle battery pack capacity and charging infrastructure for electrified public bus systems," *IEEE Trans. Transp. Electricif.*, vol. 5, no. 3, pp. 672–682, Sep. 2019.
- [10] F. He, Y. Yin, and J. Zhou, "Deploying public charging stations for electric vehicles on urban road networks," *Transp. Res. C, Emerg. Technol.*, vol. 60, pp. 227–240, Nov. 2015.
- [11] F. Xie, C. Liu, S. Li, Z. Lin, and Y. Huang, "Long-term strategic planning of inter-city fast charging infrastructure for battery electric vehicles," *Transp. Res. E, Logistics Transp. Rev.*, vol. 109, pp. 261–276, Jan. 2018.
- [12] J. He, H. Yang, T.-Q. Tang, and H.-J. Huang, "An optimal charging station location model with the consideration of electric vehicle's driving range," *Transp. Res. C, Emerg. Technol.*, vol. 86, pp. 641–654, Jan. 2018.
- [13] Y. Huang and K. M. Kockelman, "Electric vehicle charging station locations: Elastic demand, station congestion, and network equilibrium," *Transp. Res. D, Transp. Environ.*, vol. 78, Jan. 2020, Art. no. 102179.
- [14] H. Liu, Y. Zou, Y. Chen, and J. Long, "Optimal locations and electricity prices for dynamic wireless charging links of electric vehicles for sustainable transportation," *Transp. Res. E, Logistics Transp. Rev.*, vol. 152, Aug. 2021, Art. no. 102187.
- [15] K. Tiaprasert, Y. Zhang, C. Aswakul, J. Jiao, and X. Ye, "Closed-form multiclass cell transmission model enhanced with overtaking, lane-changing, and first-in first-out properties," *Transp. Res. C, Emerg. Technol.*, vol. 85, pp. 86–110, Dec. 2017.
- [16] T. Oda, M. Aziz, T. Mitani, Y. Watanabe, and T. Kashiwagi, "Mitigation of congestion related to quick charging of electric vehicles based on waiting time and cost–benefit analyses: A Japanese case study," *Sustain. Cities Soc.*, vol. 36, pp. 99–106, Jan. 2018.
- [17] E. Yao, X. Wang, Y. Yang, L. Pan, and Y. Song, "Traffic flow estimation based on toll ticket data considering multitype vehicle impact," *J. Transp. Eng., A, Syst.*, vol. 147, no. 2, Feb. 2021, Art. no. 04020158.
- [18] Y. Yang, E. Yao, Z. Yang, and R. Zhang, "Modeling the charging and route choice behavior of BEV drivers," *Transp. Res. C, Emerg. Technol.*, vol. 65, pp. 190–204, Apr. 2016.
- [19] P. Morrissey, P. Weldon, and M. O'Mahony, "Informing the strategic rollout of fast electric vehicle charging networks with user charging behavior data analysis," *Transp. Res. Rec., J. Transp. Res. Board*, vol. 2572, no. 1, pp. 9–19, Jan. 2016.
- [20] Z. Liu and Z. Song, "Network user equilibrium of battery electric vehicles considering flow-dependent electricity consumption," *Transp. Res. C, Emerg. Technol.*, vol. 95, pp. 516–544, Oct. 2018.
- [21] P. H. Divshali and C. Evans, "Behaviour analysis of electrical vehicle flexibility based on large-scale charging data," in *Proc. IEEE Milan PowerTech*, Milan, Italy, Jun. 2019, pp. 1–6.
- [22] G. Ferro, R. Minciardi, and M. Robba, "A user equilibrium model for electric vehicles: Joint traffic and energy demand assignment," *Energy*, vol. 198, May 2020, Art. no. 117299.
- [23] R. Bi, J. Xiao, V. Viswanathan, and A. Knoll, "Influence of charging behaviour given charging station placement at existing petrol stations and residential car park locations in Singapore," *Proc. Comput. Sci.*, vol. 80, pp. 335–344, Jan. 2016.
- [24] L. Hu, J. Dong, and Z. Lin, "Modeling charging behavior of battery electric vehicle drivers: A cumulative prospect theory based approach," *Transp. Res. C, Emerg. Technol.*, vol. 102, pp. 474–489, May 2019.
- [25] P. Ashkrof, G. H. de Almeida Correia, and B. van Arem, "Analysis of the effect of charging needs on battery electric vehicle drivers' route choice behaviour: A case study in The Netherlands," *Transp. Res. D, Transp. Environ.*, vol. 78, Jan. 2020, Art. no. 102206.
- [26] M. Mubarak, H. Üster, K. Abdelghany, and M. Khodayar, "Strategic network design and analysis for in-motion wireless charging of electric vehicles," *Transp. Res. E, Logistics Transp. Rev.*, vol. 145, Jan. 2021, Art. no. 102179.
- [27] W. Tu, Q. Li, Z. Fang, S. Shaw, B. Zhou, and X. Chang, "Optimizing the locations of electric taxi charging stations: A spatial-temporal demand coverage approach," *Transp. Res. C, Emerg. Technol.*, vol. 65, pp. 172–189, Apr. 2016.
- [28] Z. Zhu, Z. Gao, J. Zheng, and H. Du, "Charging station location problem of plug-in electric vehicles," *J. Transp. Geography*, vol. 52, pp. 11–22, Apr. 2016.
- [29] E. Ucer, I. Koyuncu, M. C. Kisacikoglu, M. Yavuz, A. Meintz, and C. Rames, "Modeling and analysis of a fast charging station and evaluation of service quality for electric vehicles," *IEEE Trans. Transport. Electricif.*, vol. 5, no. 1, pp. 215–225, Mar. 2019.
- [30] Z. Wei, Y. Li, and L. Cai, "Electric vehicle charging scheme for a park-and-charge system considering battery degradation costs," *IEEE Trans. Intell. Vehicles*, vol. 3, no. 3, pp. 361–373, Sep. 2018.
- [31] H. S. Hayajneh, M. N. Bani Salim, S. Bashetty, and X. Zhang, "Optimal planning of battery-powered electric vehicle charging station networks," in *Proc. IEEE Green Technol. Conference(GreenTech)*, Apr. 2019, pp. 1–4.
- [32] L. Kou, Z. Liu, and H. Zhou, "Modeling algorithm of charging station planning for regional electric vehicle," *Mod. Electr. Power*, vol. 27, no. 4, pp. 44–48, 2010.
- [33] D. Hu, J. Zhang, and Q. Zhang, "Optimization design of electric vehicle charging stations based on the forecasting data with service balance consideration," *Appl. Soft Comput.*, vol. 75, pp. 215–226, Feb. 2019.
- [34] J. Yang, J. Dong, and L. Hu, "A data-driven optimization-based approach for siting and sizing of electric taxi charging stations," *Transp. Res. C, Emerg. Technol.*, vol. 77, pp. 462–477, Apr. 2017.
- [35] C. Guo, J. Yang, and L. Yang, "Planning of electric vehicle charging infrastructure for urban areas with tight land supply," *Energies*, vol. 11, no. 9, p. 2314, Sep. 2018.
- [36] B.-G. Choi, B.-C. Oh, S. Choi, and S.-Y. Kim, "Selecting locations of electric vehicle charging stations based on the traffic load eliminating method," *Energies*, vol. 13, no. 7, p. 1650, Apr. 2020.
- [37] Y. Li, J. Luo, C.-Y. Chow, K.-L. Chan, Y. Ding, and F. Zhang, "Growing the charging station network for electric vehicles with trajectory data analytics," in *Proc. IEEE 31st Int. Conf. Data Eng.*, Apr. 2015, pp. 1376–1387.
- [38] Y. Tao, M. Huang, and L. Yang, "Data-driven optimized layout of battery electric vehicle charging infrastructure," *Energy*, vol. 150, pp. 735–744, May 2018.
- [39] Z. Yang, M. L. Franz, S. Zhu, J. Mahmoudi, A. Nasri, and L. Zhang, "Analysis of Washington, DC taxi demand using GPS and land-use data," *J. Transp. Geography*, vol. 66, pp. 35–44, Jan. 2018.
- [40] M. Zeng, Y. Pan, D. Zhang, Z. Lu, and Y. Li, "Data-driven location selection for battery swapping stations," *IEEE Access*, vol. 7, pp. 133760–133771, 2019.
- [41] S. Micari, A. Polimeni, G. Napoli, L. Andaloro, and V. Antonucci, "Electric vehicle charging infrastructure planning in a road network," *Renew. Sustain. Energy Rev.*, vol. 80, pp. 98–108, Dec. 2017.
- [42] B. Zhou, G. Chen, T. Huang, Q. Song, and Y. Yuan, "Planning PEV fast-charging stations using data-driven distributionally robust optimization approach based on ϕ -divergence," *IEEE Trans. Transp. Electricif.*, vol. 6, no. 1, pp. 170–180, Mar. 2020.
- [43] M. J. Hodgson, "A flow-capturing location-allocation model," *Geographical Anal.*, vol. 22, no. 3, pp. 270–279, 1990.
- [44] N. Jiang and C. Xie, "Computing and analyzing mixed equilibrium network flows with gasoline and electric vehicles," *Comput.-Aided Civil Infrastruct. Eng.*, vol. 29, no. 8, pp. 626–641, 2014.
- [45] Y. Jiang, W. Y. Szeto, J. Long, and K. Han, "Multi-class dynamic traffic assignment with physical queues: Intersection-movement-based formulation and paradox," *Transportmetrica A, Transp. Sci.*, vol. 12, no. 10, pp. 878–908, 2016.
- [46] M. Li, H. Huang, and H. X. Liu, "Stochastic route choice equilibrium assignment for travelers with heterogeneous regret aversions," *J. Manage. Sci. Eng.*, vol. 3, pp. 1–15, Mar. 2018.
- [47] J. Long, W. Y. Szeto, and J. Ding, "Dynamic traffic assignment in degradable networks: Paradoxes and formulations with stochastic link transmission model," *Transportmetrica B, Transp. Dyn.*, vol. 7, no. 1, pp. 336–362, Dec. 2019.
- [48] X. Zhan and S. V. Ukkusuri, "Multiclass, simultaneous route and departure time choice dynamic traffic assignment with an embedded spatial queuing model," *Transportmetrica B, Transp. Dyn.*, vol. 7, no. 1, pp. 124–146, Dec. 2019.
- [49] Y.-Z. Lin and W.-H. Chen, "A simulation-based multiclass, multimodal traffic assignment model with departure time for evaluating traffic control plans of planned special events," *Transp. Res. Proc.*, vol. 25, pp. 1352–1379, Jan. 2017.
- [50] X. Pi, W. Ma, and Z. Qian, "A general formulation for multi-modal dynamic traffic assignment considering multi-class vehicles, public transit and parking," *Transp. Res. Proc.*, vol. 38, pp. 914–934, Jan. 2019.
- [51] M. G. H. Bell, C. M. Shield, F. Busch, and G. Kruse, "A stochastic user equilibrium path flow estimator," *Transp. Res. C, Emerg. Technol.*, vol. 5, nos. 3–4, pp. 197–210, Aug./Oct. 1997.

- [52] D. Li, M. Yang, C.-J. Jin, G. Ren, X. Liu, and H. Liu, "Multi-modal combined route choice modeling in the Maas age considering generalized path overlapping problem," *IEEE Trans. Intell. Transp. Syst.*, vol. 22, no. 4, pp. 2430–2441, Apr. 2021.
- [53] Y. Sheffi and W. B. Powell, "An algorithm for the equilibrium assignment problem with random link times," *Networks*, vol. 12, no. 2, pp. 191–207, 1982.
- [54] Y. Yang, E. Yao, M. Wang, and L. Pan, "Stochastic user equilibrium assignment model for electric vehicle under hybrid traffic condition," *China J. Highway Transp.*, vol. 28, no. 9, pp. 91–97, 2015.
- [55] Z. Qian, W. Shen, and H. M. Zhang, "System-optimal dynamic traffic assignment with and without queue spillback: Its path-based formulation and solution via approximate path marginal cost," *Transp. Res. B, Methodol.*, vol. 46, no. 7, pp. 874–893, Aug. 2012.
- [56] K. An, W. Jing, and I. Kim, "Battery-swapping facility planning for electric buses with local charging systems," *Int. J. Sustain. Transp.*, vol. 14, no. 7, pp. 489–502, Jul. 2020.
- [57] M. Mitchell, *An Introduction to Genetic Algorithms*. Cambridge, MA, USA: MIT Press, 1996.
- [58] J. Jung, J. Y. J. Chow, R. Jayakrishnan, and J. Y. Park, "Stochastic dynamic itinerary interception refueling location problem with queue delay for electric taxi charging stations," *Transp. Res. C, Emerg. Technol.*, vol. 40, no. 1, pp. 123–142, 2014.
- [59] W. Ma and Z. Qian, "On the variance of recurrent traffic flow for statistical traffic assignment," *Transp. Res. C, Emerg. Technol.*, vol. 81, pp. 57–82, Aug. 2017.
- [60] S. F. A. Batista and L. Leclercq, "Regional dynamic traffic assignment framework for macroscopic fundamental diagram multi-regions models," *Transp. Sci.*, vol. 53, no. 6, pp. 1563–1590, Nov. 2019.
- [61] K. Doan and S. V. Ukkusuri, "Dynamic system optimal model for multi-OD traffic networks with an advanced spatial queuing model," *Transp. Res. C, Emerg. Technol.*, vol. 51, pp. 41–65, Feb. 2015.
- [62] V. F. Yu, A. A. N. P. Redi, Y. A. Hidayat, and O. J. Wibowo, "A simulated annealing heuristic for the hybrid vehicle routing problem," *Appl. Soft Comput.*, vol. 53, pp. 119–132, Apr. 2017.
- [63] Y. Shi and R. Eberhart, "A modified particle swarm optimizer," in *Proc. IEEE Int. Conf. Evol. Comput. IEEE World Congr. Comput. Intell.*, May 1998, pp. 69–73.
- [64] M. Xu, Q. Meng, and K. Liu, "Network user equilibrium problems for the mixed battery electric vehicles and gasoline vehicles subject to battery swapping stations and road grade constraints," *Transp. Res. B, Methodol.*, vol. 99, pp. 138–166, May 2017.
- [65] X. Gan, H. Zhang, G. Hang, Z. Qin, and H. Jin, "Fast-charging station deployment considering elastic demand," *IEEE Trans. Transp. Electrific.*, vol. 6, no. 1, pp. 158–169, Mar. 2020.



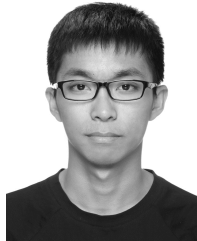
Yang Yang is currently an Assistant Professor with the School of Traffic and Transportation, Beijing Jiaotong University, Beijing, China. His research interests include travel behavior analysis and low-carbon transportation research.



Yu-Ting Zhu is currently a Lecturer with the School of E-Business and Logistics, Beijing Technology and Business University, Beijing, China. Her research interests include low-carbon transportation research, urban rail transit planning, and freight transportation optimization.



En-Jian Yao is currently a Professor with the School of Traffic and Transportation, Beijing Jiaotong University, Beijing, China. His research interests include travel behavior analysis, low-carbon transportation research, and urban rail transit planning and design.



Tian-Yu Zhang is currently pursuing the Ph.D. degree with the School of Traffic and Transportation, Beijing Jiaotong University, Beijing, China.

His research interests include low-carbon transportation research and dynamic traffic assignment.



Ke-Qi Wu is currently a Senior Engineer in transportation with the Beijing Municipal Commission of Transport, Beijing, China. Her research interests include urban planning, traffic impact analysis, urban rail transit planning, and operation organization.